Published for SISSA by Springer

Received: *July 18, 2024*
Accepted: *December 9, 2024*
Published: *February 7, 2025*

Search for resonant pair production of Higgs bosons in the $\mathrm{b\bar{b}b\bar{b}}$ final state using large-area jets in proton-proton collisions at $\sqrt{s} = 13$ TeV

The CMS collaboration

E-mail: cms-publication-committee-chair@cern.ch

Abstract: A search is presented for the resonant production of a pair of standard model-like Higgs bosons using data from proton-proton collisions at a centre-of-mass energy of 13 TeV, collected by the CMS experiment at the CERN LHC in 2016–2018, corresponding to an integrated luminosity of 138 fb^{-1}. The final state consists of two b quark-antiquark pairs. The search is conducted in the region of phase space where at least one of the pairs is highly Lorentz-boosted and is reconstructed as a single large-area jet. The other pair may be either similarly merged or resolved, the latter reconstructed using two b-tagged jets. The data are found to be consistent with standard model processes and are interpreted as 95% confidence level upper limits on the product of the cross sections and the branching fractions of the spin-0 radion and the spin-2 bulk graviton that arise in warped extradimensional models. The limits set are in the range 9.74–0.29 fb and 4.94–0.19 fb for a narrow radion and a graviton, respectively, with masses between 1 and 3 TeV. For a radion and for a bulk graviton with widths 10% of their masses, the limits are in the range 12.5–0.35 fb and 8.23–0.23 fb, respectively, for the same masses. These limits result in the exclusion of a narrow-width graviton with a mass below 1.2 TeV, and of narrow and 10%-width radions with masses below 2.6, and 2.9 TeV, respectively.

Keywords: Beyond Standard Model, Hadron-Hadron Scattering, Higgs Physics, Jets

ArXiv ePrint: 2407.13872

https://doi.org/10.1007/JHEP02(2025)040

JHEP02(2025)040

Contents

1 Introduction

In proton-proton (pp) collisions at the CERN LHC, the standard model (SM) production of a pair of Higgs bosons [1–3] involves two destructively interfering processes: the production of a virtual Higgs boson via a gluon fusion through an internal fermion loop dominated by the top quark, t, followed by an HHH vertex, and a 'box' Feynman diagram with a fermion loop resulting in two ttH vertices. Its predicted cross section of $30.8^{+6.4}_{-23.1}$ fb at a centre-of-mass energy of 13 TeV [4–13] is too small to be observable with the current data. However, according to many models "beyond the SM" (BSM), other modes of Higgs boson pair production could exist, many involving the production of a massive BSM resonance X that then decays to a Higgs boson pair ($\mathrm{X} \to \mathrm{HH}$).

Models with a warped extra dimension (WED), as proposed by Randall and Sundrum [14, 15], are among the BSM scenarios that predict the existence of resonances with large couplings to the SM Higgs boson, such as a spin-0 radion [16–18] and a spin-2 first Kaluza-Klein (KK) excitation of the graviton [19–21]. The WED models [22] postulate an additional spatial dimension l compactified between two four-dimensional hypersurfaces known as branes, with the region in between, the bulk, warped by an exponential metric κl, where κ is the warp factor. A value of $\kappa l{\approx}35$ reproduces the mass hierarchy between the Planck scale M_{Pl} and the electroweak scale [14]. One of the parameters of the model is $\kappa/\overline{M}_{\mathrm{Pl}}$, where $\overline{M}_{\mathrm{Pl}} \equiv M_{\mathrm{Pl}}/\sqrt{8\pi}$. The ultraviolet cutoff scale of the model $\Lambda_{\mathrm{R}} \equiv \sqrt{6}\mathrm{e}^{-\kappa l}\overline{M}_{\mathrm{Pl}}$ [16] is another parameter, and its value is expected to be near the TeV scale.

Searches for HH production have been performed by the ATLAS [23–34] and CMS [35–51] Collaborations using LHC pp collision data at $\sqrt{s} = 8$ and 13 TeV.

JHEP02(2025)040

A search for a KK bulk graviton or a radion decaying to HH in the $\mathrm{b\overline{b}b\overline{b}}$ final state was performed by CMS [45] using events with four separate b quark jets. A similar search targeting a higher m_X range, in which two large-area jets were used to reconstruct the highly Lorentz-boosted Higgs bosons has also been published by the CMS Collaboration [46]. The configuration of a Higgs boson candidate reconstructed as one large-area jet or as two separate narrow jets depends on its momentum [52]. A search for a new resonance X decaying to a Higgs boson and a scalar Y in the $\mathrm{b\overline{b}b\overline{b}}$ final state [53] targeted the same dijet topology in a similar kinematic regime but was optimised for a wider range of Y masses, and probed the next-to-minimal supersymmetric SM and an extension of the SM with two additional singlet scalar fields.

In this paper, we improve upon the CMS search for a high-mass resonance ($1 \leq m_\mathrm{X} \leq 3\,\mathrm{TeV}$) decaying to $\mathrm{HH} \to \mathrm{b\overline{b}b\overline{b}}$ [48] by using data collected at $\sqrt{s} = 13\,\mathrm{TeV}$ in 2016–2018, corresponding to the full Run 2 integrated luminosity of $138\,\mathrm{fb}^{-1}$. We use the scenario of ref. [54] to describe the KK graviton, where the propagation of SM fields is allowed in the bulk and follows the characteristics of the SM gauge group, with the right-handed top quark localised near the TeV brane. The theoretical values of $\sigma(\mathrm{pp} \to \mathrm{X})\mathcal{B}(\mathrm{X} \to \mathrm{HH} \to \mathrm{b\overline{b}b\overline{b}})$ are calculated for various masses, using $\Lambda_\mathrm{R} = 3\,\mathrm{TeV}$ for the radions and $\kappa/\overline{M}_\mathrm{Pl} = 0.5$ for the bulk gravitons. For these values of $\kappa/\overline{M}_\mathrm{Pl}$ and Λ_R, the branching fractions $\mathcal{B}(\mathrm{X} \to \mathrm{HH} \to \mathrm{b\overline{b}b\overline{b}})$ are 10% and 23%, for the bulk graviton and the radion, respectively, for masses of 1 TeV and larger (cf. figures 4.5 and 4.10 from ref. [55]).

Owing to the broad mass range explored, the $\mathrm{H} \to \mathrm{b\overline{b}}$ decay is studied using two analysis topologies. If m_X is large, both Higgs bosons are highly Lorentz-boosted and are reconstructed using large-area jets. These “fully-merged” events are then divided into two categories according to their purity. To identify the merged $\mathrm{H} \to \mathrm{b\overline{b}}$ decays, referred to henceforth as “H candidate jets”, we use a deep neural network jet classifier (“tagger”) algorithm, described in section 4. For resonances with masses in the intermediate range (0.8–1.5 TeV), the less energetic Higgs boson often does not produce a merged $\mathrm{b\overline{b}}$ jet, and thus these events are reconstructed using one large-area jet and a combination of two separate b quark jets (“semi-resolved” category). The inclusion of the semi-resolved events leads to an improvement in the search sensitivity for resonances with m_X around 1 TeV.

The two dominant sources of the SM background are multijet production and top quark pair production in association with jets, referred to here as $\mathrm{t\overline{t}}$+jets. Both backgrounds are estimated from data, but the procedures are assisted by simulations. To predict the multijet background, the events that fail the $\mathrm{H} \to \mathrm{b\overline{b}}$ identification of the leading-p_T jet are also used. To aid in the modelling of the $\mathrm{t\overline{t}}$+jets background, two categories enriched in $\mathrm{t\overline{t}}$+jets are defined in addition to three signal categories. For all five categories, each composed of two regions with events that pass and fail the $\mathrm{H} \to \mathrm{b\overline{b}}$ jet identification, the background estimation (described in section 5) is based on a two-dimensional fit of the reconstructed resonance mass and the mass of the leading-p_T large-area jet. In this joint binned likelihood fit of ten regions the signal strength floats unconstrained, and the nuisance parameters governing the corrections to both multijet and $\mathrm{t\overline{t}}$+jets backgrounds are floating within allowed ranges. Thus, the signal extraction and the entire background estimation are done simultaneously.

This paper is organised as follows: a brief description of the CMS detector is given in section 2 followed by a description of event simulation in section 3. The event selection criteria are defined in section 4, and section 5 describes the modelling of the major background processes. These are followed by section 6 on the relevant sources of systematic uncertainty and their variations allowed by the fit. Finally, the results are presented in section 7.

Tabulated results are provided in the HEPData record for this analysis [56].

2 The CMS detector and event reconstruction

The central feature of the CMS apparatus is a superconducting solenoid of 6 m internal diameter, providing a magnetic field of 3.8 T. Within the solenoid volume are a silicon pixel and strip tracker, a lead tungstate crystal electromagnetic calorimeter (ECAL), and a brass and scintillator hadron calorimeter (HCAL), each composed of a barrel and two endcap sections. Forward calorimeters, made of steel and quartz fibres, extend the pseudorapidity (η) coverage provided by the barrel and endcap detectors. Muons are detected in gas-ionization chambers embedded in the steel flux-return yoke outside the solenoid. A more detailed description of the CMS detector, together with a definition of the coordinate system used and the relevant kinematic variables, can be found in ref. [57].

Events of interest are selected using a two-tiered trigger system. The first level (L1), composed of custom hardware processors, uses information from the calorimeters and muon detectors to select events at a rate of around 100 kHz within a fixed latency of 4 μs [58]. The second level, known as the high-level trigger (HLT), consists of a farm of processors running a version of the full event reconstruction software optimised for fast processing, and reduces the event rate to around 1 kHz before data storage [59].

A particle flow (PF) algorithm [60] aims to reconstruct and identify each individual particle in an event (PF candidate), with an optimised combination of information from the various elements of the CMS detector. The energy of photons is obtained from the ECAL measurement. The energy of electrons is determined from a combination of the track momentum at the primary interaction vertex, the corresponding ECAL cluster energy, and the energy sum of all bremsstrahlung photons attached to the track. The momentum of muons is obtained from the curvature of the corresponding track. The energy of charged hadrons is determined from a combination of their momentum measured in the tracker and the matching ECAL and HCAL energy deposits, corrected for zero-suppression effects and for the response function of the calorimeters to hadronic showers. Finally, the energy of neutral hadrons is obtained from the corresponding corrected ECAL and HCAL energies. The primary vertex (PV) is taken to be the vertex corresponding to the hardest scattering in the event, evaluated using tracking information alone, as described in section 9.4.1 of ref. [61].

For each event, jets are clustered from these reconstructed particles using the anti-k_{T} algorithm [62, 63] with a distance parameter of 0.4 (AK4 jets) or 0.8 (AK8 jets). Jet momentum is determined as the vectorial sum of all particle momenta in the jet, and is found from simulation to be, on average, within 5 to 10% of the true momentum over the whole transverse momentum (p_{T}) spectrum and detector acceptance. Additional pp interactions within the same or nearby bunch crossings (pileup) can contribute additional tracks and calorimetric energy depositions, increasing the apparent jet momentum. To mitigate this effect, tracks identified to be originating from pileup vertices are discarded, and an offset correction is applied to correct for remaining contributions [64, 65]. Jet energy corrections

JHEP02(2025)040

are derived from simulation studies so that the average measured energy of jets becomes identical to that of particle level jets. In situ measurements of the momentum balance in dijet, photon+jet, Z+jet, and multijet events are used to determine any residual differences between the jet energy scale in data and in simulation, and appropriate corrections are made [66]. Additional selection criteria are applied to each jet to remove jets arising from instrumental effects or reconstruction failures [67]. The jet energy resolution amounts typically to 15–20% at 30 GeV, 10% at 100 GeV, and 5% at 1 TeV [66].

3 Event simulation

Two scenarios of bulk graviton and radion signal events are considered: "narrow-width" signal shapes with a width of 1 MeV and a "10%-width" where the width is set to 10% of the resonance mass. The width of 1 MeV is much smaller than the standard deviation of the dijet invariant mass distribution ($\sim$5%, in the considered mass range 1–3 TeV) and thus the narrow-width scenario provides a limiting case where the signal shape is completely determined by the experimental resolution. A width of 10% was chosen to demonstrate the effects of a resonance width larger than the jet mass resolution. Although the background estimation would be valid for much broader signals, the analysis is not optimised for them. All signals are simulated at leading order (LO) in the mass range 1–3 TeV, using the MadGraph5_aMC@NLO event generator [68]; version 2.2.2 is used for the 2016 data-taking period, and 2.4.2 for 2017 and 2018. The NNPDF3.0 LO parton distribution function (PDF) set [69], taken from LHAPDF6 library [70–73], with the four-flavour scheme, is used for all signal samples. The parton shower and hadronization are simulated with pythia 8.212 [74].

The dominant background consists of events composed primarily of jets (multijet events) arising from the SM quantum chromodynamics (QCD) interaction, and is modelled from data. The $\mathrm{t\bar{t}}$+jets events comprise most of the remaining background and are generated at next-to-LO using powheg 2.0 [75–77] using NNPDF3.0 LO PDF set for 2016 data-taking period, and PDF4LHC15 next-to-next-to-LO (NNLO) PDF set [69, 70, 73, 78–80] to model data from 2017 and 2018. These events are showered by pythia 8, using the CUETP8M2T4 tune [81, 82]. The contribution from $\mathrm{t\bar{t}}$+jets is estimated using a NNLO cross section of 832^{+46}_{-52} pb [83], corresponding to the top quark mass of 172.5 GeV. To account for the difference in the shape of the p_{T} distribution of the top quarks between data and simulation, arising from the absence of the contribution from the NNLO diagrams, the simulated $\mathrm{t\bar{t}}$+jets events are reweighted using the p_{T}-dependent scale factor, $\mathrm{e}^{\alpha-\beta p_{\mathrm{T}}}$, with $\alpha = 0.0615$ and $\beta = 0.0005$, derived from low-p_{T} $\mathrm{t\bar{t}}$+jets events. A sample of multijet events from QCD interactions, simulated at LO using MadGraph5_aMC@NLO and pythia 8, and NNPDF3.0 (for 2016) or PDF4LHC15 (for 2017 and 2018) is used to develop and validate the background estimation techniques prior to being applied to the data. Other background processes, such as WZ, $\mathrm{t\bar{t}Z}$ or Z+jets production, are also considered but their yields are found to be negligible.

All generated samples are processed through a Geant4-based [84, 85] simulation of the CMS detector. The effect of pileup, averaging 23–32 additional interactions per bunch crossing, for the LHC beam conditions between 2016 and 2018, is included in the simulations, and the samples are reweighted to match the distribution of the number of pp interactions observed in the data, assuming a total inelastic pp collision cross section of 69.2 mb [86].

JHEP02(2025)040

Variable	Selection
Leading two AK8 jets	$p_{\mathrm{T}} > 300\,\mathrm{GeV}$ and $\lvert\eta\rvert < 2.4$
$\lvert\Delta\eta\rvert$	<1.3
Sub-leading AK8 jet soft-drop mass	$110 < m_{\mathrm{SD}} < 140\,\mathrm{GeV}$
$m_{\mathrm{HH,corr}}$	$>750\,\mathrm{GeV}$

Table 1. Event selection criteria for the fully-merged topology.

4 Event selection

Collision events are selected using a logical OR of triggers based on the jet activity in the event. One trigger path requires that the p_{T} sum of all AK4 jets in the event (H_{T}) be greater than 800, 900, or 1050 GeV, depending on the data collection year and the LHC beam instantaneous luminosity. A second trigger path collects events with $H_{\mathrm{T}} > 650\,\mathrm{GeV}$, and with a pair of AK4 jets that has invariant mass above 900 GeV and a pseudorapidity separation $\lvert\Delta\eta\rvert < 1.5$. A third trigger path accepts events if the p_{T} of the leading AK8 jet is greater than 360 or 400 GeV (depending on the data collection year) and the "trimmed mass" of an AK8 jet is above 30 GeV. The jet trimmed mass is obtained after removing remnants of soft radiation with the jet trimming technique [87], using a subjet size parameter of 0.3 and a subjet-to-AK8 jet p_{T} fraction of 0.1.

Offline, collected events are split into three categories: one semi-resolved category and two fully-merged categories, further separated by purity. Since the background estimation uses the mass and the $\mathrm{H} \to \mathrm{b\bar{b}}$ jet tagger discriminant of the leading-p_{T} AK8 jet, the events are not preselected based on these variables. The AK8 jets are required to have $\lvert\eta\rvert < 2.4$, and $p_{\mathrm{T}} > 300\,\mathrm{GeV}$. The fully-merged categories require two such AK8 jets (each representing a Higgs boson candidate), whereas the semi-resolved category requires only one, with the other Higgs boson candidate reconstructed from a pair of b-tagged AK4 jets.

A resonant HH signal of high mass results in a small $\lvert\Delta\eta\rvert$ between the two Higgs bosons, while the multijet background often produces events with larger values of $\lvert\Delta\eta\rvert$. Events in the fully-merged category are therefore required to have $\lvert\Delta\eta\rvert < 1.3$ between the H candidate jets. The subleading AK8 jet is required to have its soft-drop mass, the jet mass that results from applying the soft-drop algorithm [88, 89], between 110–140 GeV, consistent with the Higgs boson mass, $m_{\mathrm{H}} = 125\,\mathrm{GeV}$ [90, 91]. The fully-merged selection is summarised in table 1.

A deep neural network based tagger, "DeepAK8" [92], is used to identify the boosted $\mathrm{H} \to \mathrm{b\bar{b}}$ candidate jets. We use a "mass-decorrelated" version of this tagger, which exploits an adversarial network to reduce the correlation of the tagging score with the soft-drop jet mass [92]. A significantly reduced sculpting of the distribution of the H candidate's jet mass preserves its sidebands and allows the use of the jet mass in conjunction with the DeepAK8 tagger in the background estimate. The efficiency of the DeepAK8 tagger is calibrated in data using a sample of jets originating from gluons splitting into $\mathrm{b\bar{b}}$ pairs that produce merged jets. A jet in this sample must have a soft-drop mass in the 50-200 GeV range and have two secondary vertices, each matched to one subjet. This selection results in tagger distributions that are similar between the sample jets and the signal $\mathrm{H} \to \mathrm{b\bar{b}}$ jets.

JHEP02(2025)040

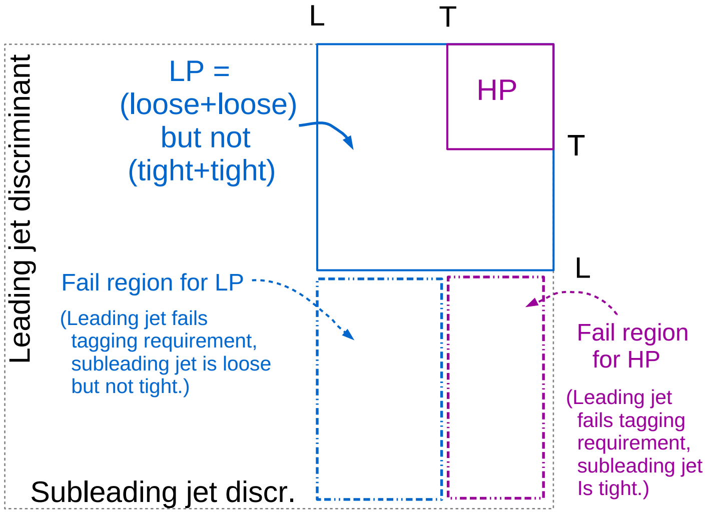

Figure 1. A diagram showing high-purity (HP, purple) and low-purity (LP, blue) pass regions (solid) and their corresponding fail regions (dash-dotted).

The DeepAK8 tagger data-to-simulation correction factors range from 0.9 to 1.4, depending on the jet p_{T} and data-taking year [93]. The DeepAK8 tagger outperforms the "double-b" $\mathrm{H} \to \mathrm{b\bar{b}}$ tagger used previously [48], resulting in an increase of the sensitivity from the tagger alone by a factor of $\approx$2.5 over the whole search domain.

The AK8 jets with DeepAK8 tagger discriminant above 0.8 are said to pass a "loose" criterion while those with the discriminant above 0.9 pass the "tight" criterion. The efficiency of the tight criterion for H candidate jets from a 1500 GeV narrow radion signal is about 60%, with a misidentification probability of QCD jets of 1%. For jets that pass the loose but not tight criterion, the H jet efficiency is about 20%, with the misidentification probability of 2%. The fully-merged events are split into two categories based on the purity of the H candidate jets: events are categorised as either "high purity" (HP), where both AK8 jets satisfy the tight threshold, or as "low purity" (LP), where both AK8 jets pass the loose tagging threshold but are not part of the HP category.

We denote the signal regions as "pass" regions. For the purpose of background estimation, for each signal region we also define a control region where the leading-p_{T} AK8 jet fails the tagging requirement; we denote them as "fail" regions, and define them separately for HP and LP categories. In defining the mutually exclusive HP and LP fail regions, we aim to model the signal regions with events that have the same criteria for the subleading jet, which makes them kinematically similar. The HP fail region (used to predict the background in the HP signal region) is defined by the leading-p_{T} H candidate jet failing the loose tagger requirement, while the subleading-p_{T} H candidate jet passes the tight DeepAK8 tagger requirement. Analogously, the LP fail region is defined by the leading H candidate jet failing the loose criterion while the subleading passes it, but fails the tight one. A schematic diagram of these four regions is shown in figure 1. The HP selection corresponds to a signal efficiency of 7–11% for a narrow radion signal for masses m_{X} in the range 1–3 TeV, and slightly higher for the bulk graviton. The LP selection results in signal efficiencies of 3–4% over the same m_{X} domain.

Two dedicated $t\bar{t}$+jets event control regions (each consisting of corresponding HP and LP events) are also used to correct the modelling of the $t\bar{t}$+jets background component for events with high jet p_T, for which the $t\bar{t}$ simulation does not agree with data. The $t\bar{t}$ control regions use the same selections as the HP and LP categories, except for a window on the soft-drop mass of the subleading-p_T jet, which is shifted from $110 < m_{SD} < 140$ to $140 < m_{SD} < 210\,\text{GeV}$ in order to correspond to the top quark mass.

Events that fail the fully-merged selection for either HP or LP category are considered in the semi-resolved selection. Jets for the semi-resolved category are required to have $|\eta| < 2.4$, and $p_T > 30\,\text{GeV}$ (300 GeV) for AK4 (AK8) jets.

To find a Higgs boson decay into two resolved b quark jets, all AK4 jets in each event are examined by the "DeepJet" algorithm [94, 95], which gives the probability for a jet to have originated from a bottom quark. DeepJet is a neural network trained using information from tracks and secondary vertices associated with the jet.

The DeepJet selection on AK4 jets uses the "medium" working point, which corresponds to a 1% mistag rate for gluon and light-flavoured quark jets. It results in a b tagging efficiency of about 70% for b quark jets in the p_T range 80–150 GeV, and decreasing to about 50% for $p_T \approx 1000\,\text{GeV}$. The b tagging efficiency in the simulation is corrected to match that in the data, using measurements of the b-tagging algorithm performance in a sample of muon-enriched jets and b jets from $t\bar{t}$+jets events, with the correction factor ranging from 0.95 to 1.1 [95].

Resolved $H \to b\bar{b}$ candidates are constructed by considering all pairs of b-tagged AK4 jets. Events are required to have least one pair where both AK4 jets (jets "j_2" and "j_3") are separated by $\Delta R = \sqrt{(\Delta\phi)^2 + (\Delta\eta)^2} > 0.8$ (where ϕ is the azimuthal angle in radians) from the leading-p_T AK8 jet (jet "J_1") and are within $\Delta R < 1.5$ of each other. If several such pairs are found, the pair of jets j_2 and j_3 that has the highest sum of the AK4 jet DeepJet discriminant values is selected. The invariant mass of j_2 and j_3, $m_{j_2j_3}$, is required to be within 90–140 GeV, forming the resolved $H \to b\bar{b}$ candidate. The leading-p_T AK8 jet is then identified as the merged H candidate, and the pair of AK4 jets is identified as the resolved H candidate. If no resolved H candidate is found starting from the leading-p_T AK8 jet, then this process is repeated with the subleading-p_T AK8 jet as a merged H candidate. The event is rejected if a $H \to b\bar{b}$ pair is not found even in this case. As in the fully-merged regime, the events are required to have a pseudorapidity difference between the two H candidates $|\Delta\eta| < 1.3$.

In the semi-resolved category, the "pass" region is defined by the leading-p_T AK8 jet having a DeepAK8 tagger discriminant above 0.9, and the "fail" region below 0.9. The efficiency of the semi-resolved selection peaks at ≈3.5% around 1.2–1.4 TeV, depending on the signal, and rapidly falls at higher m_X masses. The requirements for the semi-resolved events are summarised in table 2.

The main variable used in the search for an HH resonance is the "corrected HH mass". For the fully-merged categories it is defined as $m_{HH,corr} \equiv m_{JJ} + (m_H - m_{J_1}) + (m_H - m_{J_2})$, where m_{JJ} is the dijet invariant mass, m_{J_1} and m_{J_2} are the soft-drop masses of the leading and subleading H candidate jets in the event, and $m_H = 125\,\text{GeV}$ is the nominal Higgs boson mass. In the semi-resolved analysis, this quantity is defined by $m_{HH,corr} \equiv m_{Jjj} +$

Variable	Selection
Leading AK8 jet	$p_{\mathrm{T}} > 300\,\mathrm{GeV}$ and $\lvert\eta\rvert < 2.4$
AK4 jets	$p_{\mathrm{T}} > 30\,\mathrm{GeV}$ and $\lvert\eta\rvert < 2.4$
$\lvert\Delta\eta\rvert$	<1.3
DeepJet	Medium working point
Invariant mass of two AK4 jets	$90 < m_{\mathrm{j_2j_3}} < 140\,\mathrm{GeV}$
$m_{\mathrm{HH,corr}}$	>750 GeV

Table 2. Event selection criteria for the semi-resolved topology.

$(m_{\mathrm{H}} - m_{\mathrm{J_1}}) + (m_{\mathrm{H}} - m_{\mathrm{j_2j_3}})$, where m_{Jjj} is the invariant mass of the three jets comprising a semi-resolved HH candidate. The corrected HH mass is used rather than the invariant mass of the two reconstructed H candidates because effects due to fluctuations in jet reconstruction or to missing p_{T} associated with a neutrino from a b quark decay are correlated between the H jet mass and the invariant mass of the HH system. Adjusting the $\mathrm{H} \to \mathrm{b\overline{b}}$ candidates to the nominal H mass improves our estimate of the HH invariant mass. Using the corrected HH mass leads to an 8–10% improvement in the invariant jet mass resolution [46]. A requirement of $m_{\mathrm{HH,corr}} > 750\,\mathrm{GeV}$ is applied for selecting signal-like events because of trigger turn-on effects.

5 Background model

The background is predicted to be dominated by multijet and $\mathrm{t\overline{t}}$+jets production. The contribution from processes like WZ, $\mathrm{t\overline{t}Z}$ or Z+jets production was found to be negligible. The total background model is constructed as a sum of the individual background contributions using a Poisson distribution for each bin of the two-dimensional $(m_{\mathrm{J_1}}, m_{\mathrm{HH,corr}})$ distribution. The H candidate jet mass is used as one of the discriminants because the signal and the $\mathrm{t\overline{t}}$+jets background exhibit shapes distinct from each other and from the multijet background. To extract the signal, we compare the number of expected events from both the background-only and signal-plus-background hypotheses with the number of observed events in data using a likelihood ratio fit. The number of extracted signal events can then be related to the production cross section via $N_{\text{signal}} = \sigma_X \mathcal{B}(\mathrm{X} \to \mathrm{HH} \to \mathrm{b\overline{b}b\overline{b}})\varepsilon L$, where σ_X is the production cross section of X (a radion or a bulk graviton), $\mathcal{B}(\mathrm{X} \to \mathrm{HH} \to \mathrm{b\overline{b}b\overline{b}})$ is the product of the branching fractions of $\mathrm{X} \to \mathrm{HH}$ and the two $\mathrm{H} \to \mathrm{b\overline{b}}$ decays, ε is the product of the acceptance and the efficiency to reconstruct an HH event, and L is the integrated luminosity of the data set.

The multijet background estimation relies on a "pass-to-fail ratio", a transfer function between the pass and fail regions defined in section 4 and determined by the discriminant of the leading-p_{T} H candidate jet. In this analysis, the pass-to-fail ratio is of the order of 10^{-2}. Conceptually, the pass-to-fail ratio is measured in the Higgs boson mass sidebands ($m_{\mathrm{J_1}} < 100\,\mathrm{GeV}$ and $m_{\mathrm{J_1}} > 140\,\mathrm{GeV}$) and interpolated into the signal region ($100 < m_{\mathrm{J_1}} < 140\,\mathrm{GeV}$); however, both steps are done simultaneously with the extraction of the signal yield and profiling over all nuisance parameters, including those that govern the normalizations and shapes of the $\mathrm{t\overline{t}}$+jets component.

JHEP02(2025)040

The $\mathrm{t\bar{t}}$+jets contributions to the signal categories are obtained from simulation, but their overall normalization and their shapes are allowed to be modified by nuisance parameters that are described in the next section. These nuisance parameters are constrained using two control event categories enriched in $\mathrm{t\bar{t}}$+jets, which are also a part of the joint likelihood. Therefore, both the signal and all backgrounds are simultaneously obtained from a one-step fit to the $(m_{\mathrm{J_1}}, m_{\mathrm{HH,corr}})$ planes in the ten pass and fail regions.

The total numbers of expected events failing, n_{F}, and passing, n_{P}, the DeepAK8 tagger requirement are given by

$$n_{\mathrm{F}}(i,\vec{\theta}) = n_{\mathrm{F}}^{\mathrm{QCD}}(i) + n_{\mathrm{F}}^{\mathrm{t\bar{t}}}(i,\vec{\theta}) + n_{\mathrm{F}}^{\mathrm{X}}(i,\vec{\theta}) \tag{5.1}$$

and

$$n_{\mathrm{P}}(i,\vec{\theta}) = n_{\mathrm{P}}^{\mathrm{QCD}}(i) + n_{\mathrm{P}}^{\mathrm{t\bar{t}}}(i,\vec{\theta}) + n_{\mathrm{P}}^{\mathrm{X}}(i,\vec{\theta}) \tag{5.2}$$

where i is a bin in the 2D $(m_{\mathrm{J_1}}, m_{\mathrm{HH,corr}})$ plane, and $\vec{\theta}$ is the set of all nuisance parameters that quantify the systematic uncertainties, as described in section 6. Each bin in the "fail" 2D distribution, $n_{\mathrm{F}}^{\mathrm{QCD}}(i)$, is represented by an individual parameter in the fit that is required to be positive but is otherwise unconstrained.

The predicted multijet yield in the "pass" 2D distribution, $n_{\mathrm{P}}^{\mathrm{QCD}}(i)$, is obtained by

$$n_{\mathrm{P}}^{\mathrm{QCD}}(i) = n_{\mathrm{F}}^{\mathrm{QCD}}(i)\, R_{\mathrm{P/F}}(m_{\mathrm{J_1}}, m_{\mathrm{HH,corr}}) \tag{5.3}$$

where $R_{\mathrm{P/F}}(m_{\mathrm{J_1}}, m_{\mathrm{HH,corr}})$ is the transfer function.

We define the transfer functions in data and in the QCD multijet simulation as $R_{\mathrm{P/F}}^{\mathrm{data}}(m_{\mathrm{J_1}}, m_{\mathrm{HH,corr}})$ and $R_{\mathrm{P/F}}^{\mathrm{sim}}(m_{\mathrm{J_1}}, m_{\mathrm{HH,corr}})$, respectively. The $R_{\mathrm{P/F}}^{\mathrm{data}}(m_{\mathrm{J_1}}, m_{\mathrm{HH,corr}})$ and $R_{\mathrm{P/F}}^{\mathrm{sim}}(m_{\mathrm{J_1}}, m_{\mathrm{HH,corr}})$ both vary smoothly as a function of $m_{\mathrm{J_1}}$ and $m_{\mathrm{HH,corr}}$ because HH candidates in multijet processes arise from random combinations of jets. The data-to-simulation ratio of these 2D functions,

$$R_{\mathrm{ratio}}(m_{\mathrm{J_1}}, m_{\mathrm{HH,corr}}) \equiv \frac{R_{\mathrm{P/F}}^{\mathrm{data}}(m_{\mathrm{J_1}}, m_{\mathrm{HH,corr}})}{R_{\mathrm{P/F}}^{\mathrm{sim}}(m_{\mathrm{J_1}}, m_{\mathrm{HH,corr}})}, \tag{5.4}$$

is therefore also smooth and can be parameterised with an analytic function of $m_{\mathrm{J_1}}$ and $m_{\mathrm{HH,corr}}$.

While $R_{\mathrm{P/F}}^{\mathrm{data}}(m_{\mathrm{J_1}}, m_{\mathrm{HH,corr}})$ could also be described by analytic functions, features of this shape that are hard to model analytically can be factored out by using the QCD simulation, and the fit of the analytic function to data is only responsible for describing the residual differences between data and simulation that can be parameterised with fewer parameters than the shape of $R_{\mathrm{P/F}}^{\mathrm{data}}(m_{\mathrm{J_1}}, m_{\mathrm{HH,corr}})$. Thus the number of events in a given bin of the passing region is obtained from

$$n_{\mathrm{P}}^{\mathrm{QCD}}(i) = n_{\mathrm{F}}^{\mathrm{QCD}}(i)\, R_{\mathrm{P/F}}^{\mathrm{sim}}(m_{\mathrm{J_1}}, m_{\mathrm{HH,corr}})\, R_{\mathrm{ratio}}(m_{\mathrm{J_1}}, m_{\mathrm{HH,corr}}) \tag{5.5}$$

where $R_{\mathrm{ratio}}(m_{\mathrm{J_1}}, m_{\mathrm{HH,corr}})$ is a surface parameterised by the product of two one-dimensional polynomials in the $(m_{\mathrm{J_1}}, m_{\mathrm{HH,corr}})$ plane with coefficients determined from the fit to data. Second-order polynomials were chosen for $R_{\mathrm{ratio}}(m_{\mathrm{J_1}}, m_{\mathrm{HH,corr}})$ parameterization, along both

Source	Effect on signal (%)	Effect on $t\bar{t}$ background (%)
Integrated luminosity	1.6	1.6
Pileup	0.1	0.2
PDF and scales	0.4	1.2
$t\bar{t}$ cross section	—	5.0
Trigger efficiency	4.0	5.7
Top quark p_T reweighting	—	13.7
DeepAK8 $H \to b\bar{b}$ efficiency	18.3	12.7
DeepJet b tagging efficiency	0.0	0.0
Jet energy scale	1.5	0.7
Jet energy resolution	0.9	0.9
Jet mass scale	1.2	0.8
Jet mass resolution	6.2	6.7

Table 3. Summary of the impact of each source of systematic uncertainty on the signal and $t\bar{t}$ background yields in the high purity signal region for a radion resonance at 1500 GeV. The impact of the same nuisance parameters in other signal regions and for other resonance masses is similar.

m_{J_1} and $m_{HH,corr}$ axes, based on a Fisher test [96], where polynomial terms were added until the p-value obtained in the test was larger than 0.05.

To reduce the effect of statistical fluctuations on the calculation of $R^{sim}_{P/F}(m_{J_1}, m_{HH,corr})$ in the QCD multijet simulation, the pass and fail distributions are smoothed using an adaptive kernel density estimate [97] prior to calculating the ratio.

6 Sources of systematic uncertainty

The following sources of systematic uncertainty affect the expected signal and background event yields. A complete list of systematic uncertainties and ranges for the associated nuisance parameters is given in table 3. These ranges are used as input to the fit, and the minimization of the likelihood further constrains some of them. None of these lead to a significant change in the signal shape and, after the fit, their impact on the signal yield is significantly smaller than the effect of limited statistics.

The uncertainties in the modelling of the trigger response are particularly important for $m_{HH,corr} < 1100$ GeV, where the trigger efficiency drops below 99%. The trigger efficiency in each category is measured in the data as a fraction of events with at least one AK4 jet with $p_T > 260$ GeV satisfying the offline selection that passes the trigger selection criteria. Simulated events are weighted by this efficiency as a function of the invariant mass of the two leading-p_T AK8 jets in the event, $m_{HH,corr}$. The trigger efficiency in simulation is corrected by a scale factor, which has an uncertainty between 1 and 15%, attributable to the control trigger inefficiency and the sample size used.

JHEP02(2025)040

The impact of the jet energy scale and resolution uncertainties [67] on the signal yields is estimated to be 1–3%, depending on the signal mass. The jet mass scale and resolution are measured using a sample of boosted $\mathrm{W} \to \mathrm{q\overline{q}'}$ jets in semileptonic $\mathrm{t\bar{t}}$ events. The jet mass scale and resolution have a 2% effect on the signal yields because of a change in the mean of the H candidate jet mass distribution.

Scale factors are used to correct the signal event yields so that their DeepAK8 tagger and DeepJet discriminant efficiencies are the same as for data. The DeepAK8 tagger and the DeepJet discriminant scale factors are taken to be 100% correlated. The associated uncertainty in the scale factor is 2–9% [93], depending on the DeepAK8 tagger working point and jet p_{T}, and is propagated to the total uncertainty in the signal yield.

The impact of the uncertainties in the renormalization and factorization scale and the parton distribution functions (PDF), the latter derived using the PDF4LHC procedure [73] and the NNPDF3.0 PDF sets, is estimated to be 0.5%. These uncertainties affect the product of the signal acceptance and the selection efficiency. The factorization scale and PDF uncertainties have negligible impact on the signal $m_{\mathrm{HH,corr}}$ distributions. Additional systematic uncertainties associated with pileup modelling (1–2%, based on a 4.6% variation on the pp total inelastic cross section [86]) and with the integrated luminosity determination [98–100] (1.6%, combining the measurements of the three years of data taking), are applied to the signal yield.

The systematic uncertainties applied to the signal are also applied to the $\mathrm{t\bar{t}}$+jets background, as appropriate. The total uncertainty in the $\mathrm{t\bar{t}}$+jets cross section is 7%. The correction to the shape of the top quark $p_{\mathrm{T}}^{\mathrm{t}}$ distribution (described in section 3) has two parts, an additional normalization correction e^{α} and a shape correction $\mathrm{e}^{-\beta p_{\mathrm{T}}^{\mathrm{t}}}$. Each correction is assigned independent multiplicative uncertainties of 2 and 0.5 times the nominal weight.

An uncertainty in the "bandwidth" parameter of the kernel density estimate, which acts as a scale for the width of the adaptive kernels, was studied by varying this parameter, and its impact is found to be negligible.

The main source of uncertainty in the multijet background estimate is the statistical uncertainty in the fit of R_{ratio}. This uncertainty, amounting to 2–10%, is fully correlated between all $m_{\mathrm{HH,corr}}$ bins. Additional statistical uncertainties in the background shape and yield in the signal region result from the finite sizes of the multijet samples in the fail region and are evaluated using the Barlow-Beeston Lite method [101, 102]. These uncertainties are small compared to the uncertainty in the $R_{\mathrm{P/F}}$ ratio, and are uncorrelated from bin to bin.

7 Results

Results are obtained using a statistical combination of the semi-resolved and fully-merged event categories. An $\mathrm{X} \to \mathrm{HH}$ signal is resonant in the 2D space of the different signal event categories, as discussed in section 5. The likelihood is formed by combining 2D binned likelihoods of ten regions: HP, LP, and semi-resolved signal categories, and HP and LP $\mathrm{t\bar{t}}$ control categories, where each category provides both a pass and a fail region. The projections of the slices of the post-fit 2D distributions in the three signal regions (HP, LP, and semi-resolved) are shown in figures 2–4.

JHEP02(2025)040

The narrow radion signal corresponding to the resonance mass of 1500 GeV is also shown. This resonance mass is chosen to illustrate the contribution of the semi-resolved category compared with the HP and LP categories; the signal is scaled by the same scale in all three figures. The sensitivity is dominated by the HP region over the whole resonance mass domain. At lower resonance masses, the semi-resolved category contributes significantly to the sensitivity of the search. The LP category contributes only at very high resonance masses, where the standard model backgrounds are low.

The three signal regions are examined for an excess of events above the predicted background, and the data are found to be consistent with the expected background predictions. We proceed to set an upper limit on the number of possible signal events in our data.

Upper limits at 95% confidence level (CL) are set on the product of the production cross section and the branching fractions, $\sigma(\mathrm{pp} \to \mathrm{X})\mathcal{B}(\mathrm{X} \to \mathrm{HH} \to \mathrm{b\bar{b}b\bar{b}})$. They are obtained using the profile likelihood as a test statistic [103]. The systematic uncertainties are treated as nuisance parameters and are profiled in the minimization of the negative of the logarithm of the profile likelihood ratio, and the distributions of the likelihood ratio are calculated using the asymptotic approximation [104] of the procedure reported in refs. [105, 106].

As shown in figure 5 (left) a narrow radion with mass between 1–2.6 TeV is excluded at 95% CL for the assumed value of the cutoff scale, $\Lambda_\mathrm{R} = 3\,\mathrm{TeV}$. A narrow bulk graviton for the assumed value of the ultraviolet cutoff scale, $k/\overline{M}_\mathrm{Pl} = 0.5$, is excluded at 95% CL only for masses between 1–1.2 TeV, as shown in figure 5 (right). The deviations in the observed limits at graviton and radion masses of 1.3 and 1.5 TeV, respectively, correspond to a small upward fluctuation of data over the background prediction at $m_\mathrm{HH,corr} \approx 1.4\,\mathrm{TeV}$, visible in figure 2, middle row. The corresponding exclusion limits, assuming a signal with 10% decay width, are shown in figure 6. The product of the efficiency and the acceptance for the 10%-width signals is 3–5% lower than for the narrow signals, and, consequently, the cross section exclusion limits are similar.

These limits result in the exclusion of the narrow-width graviton with m_X below 1.2 TeV. Narrow and 10%-width radion with masses below 2.6 TeV, and 2.9 TeV, respectively, are also excluded. This is a substantial improvement over the previous CMS radion exclusion limit of ≈1.6 TeV [48]. The analysis presented in this paper complements a previous result from ATLAS that achieved an almost identical sensitivity for $X \to \mathrm{HH} \to 4\mathrm{b}$ for both spin-0 and spin-2 hypotheses [33] between 1.5–3 TeV, while employing a different background estimation strategy and H jet identification. Below 1.5 TeV the ATLAS analysis benefits from the combination with the fully resolved 4b channel.

8 Summary

A search has been presented for the pair production of standard model Higgs bosons (HH) from the decay of a spin-0 radion or a spin-2 bulk graviton as predicted in warped extradimensional models, using data from proton-proton collisions at a centre-of-mass energy of 13 TeV and corresponding to an integrated luminosity of $138\,\mathrm{fb}^{-1}$.

The search is restricted to the case where each Higgs boson decays to a bottom quark-antiquark pair. It is conducted in the region of phase space where at least one of the Higgs bosons has a large Lorentz boost, so that the $\mathrm{H} \to \mathrm{b\bar{b}}$ decay products are collimated to form

JHEP02(2025)040

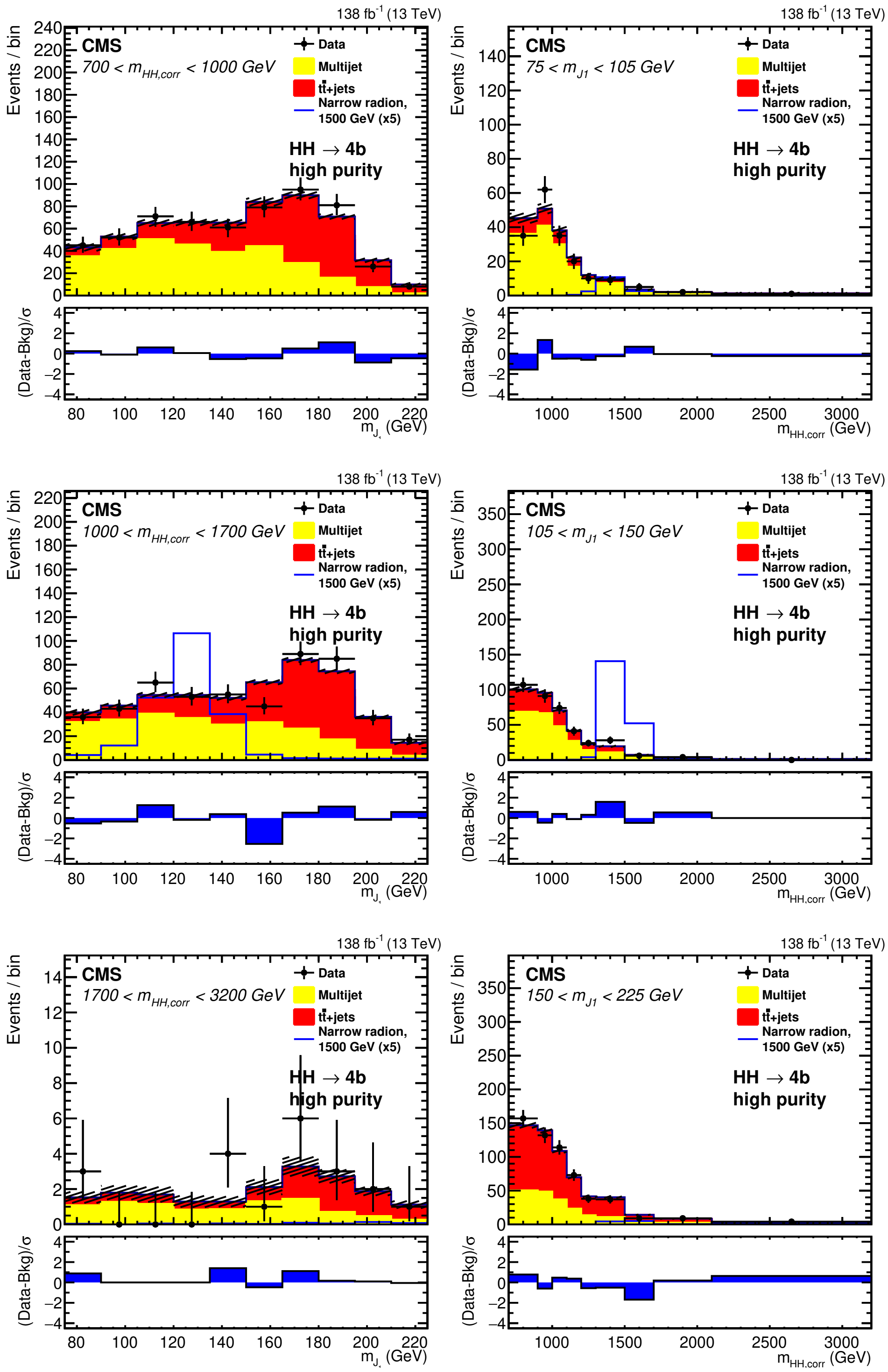

Figure 2. Slices of 2D distributions of observed events and the post-fit templates in the HP signal region, projected onto the plane of leading jet mass m_{J_1} (left) and corrected HH mass $m_{\mathrm{HH,corr}}$ (right) axes, together with the signal (scaled up by a factor of five) expected for a radion of mass 1.5 TeV. For this and following figures, the value of σ in the lower panel is $\sigma = \sqrt{\sigma^2_{\mathrm{bkg}} + \sigma^2_{\mathrm{data}}}$, where σ_{bkg} is the total post-fit uncertainty in the background and σ_{data} is the statistical uncertainty associated with the number of data events in a particular bin.

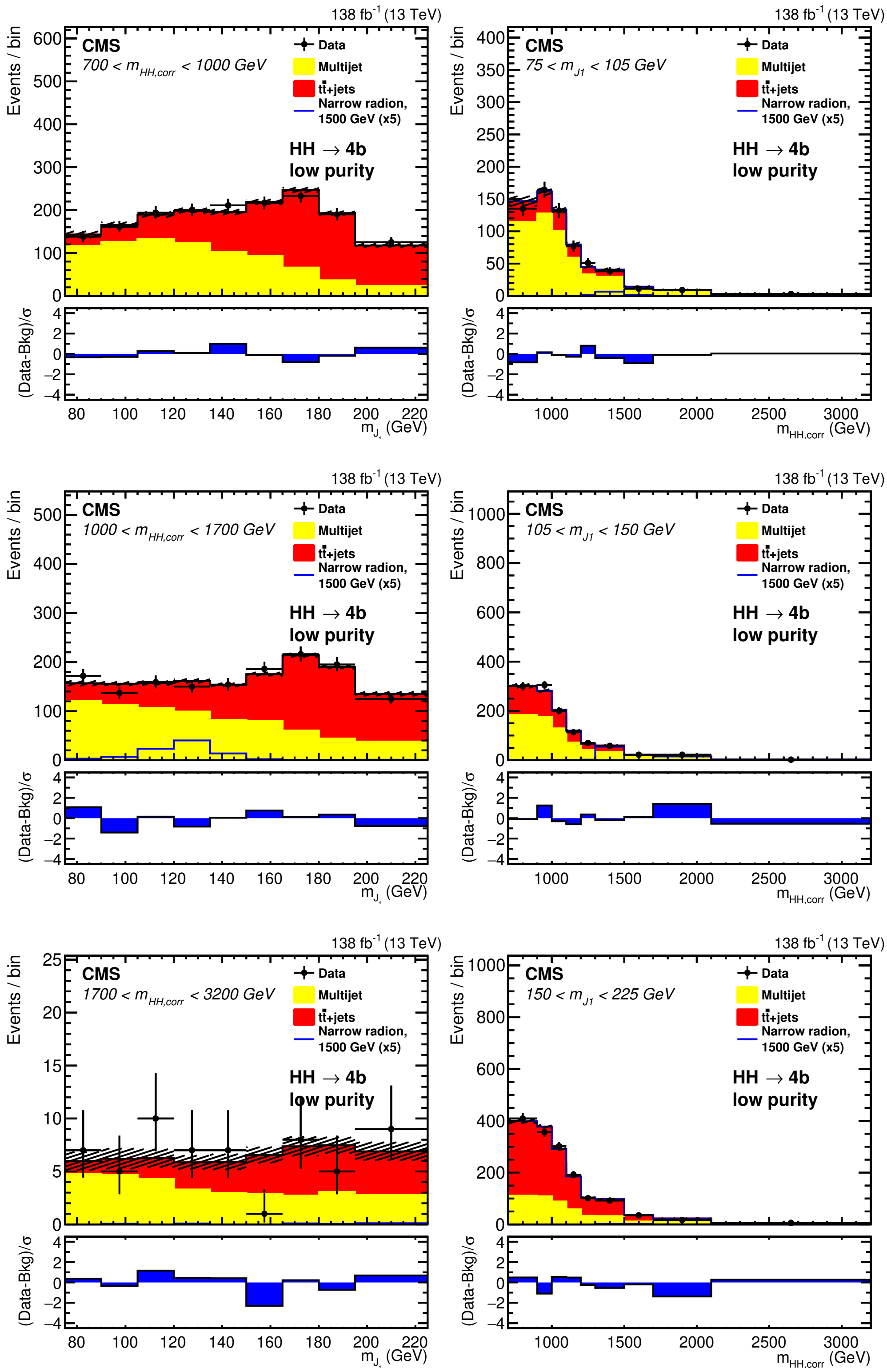

Figure 3. Slices of 2D distributions of observed events and the post-fit templates in the LP signal region, projected onto the m_{J_1} (left) and $m_{\mathrm{HH,corr}}$ (right) axes, together with the signal expected for a radion of mass 1.5 TeV. The signal is scaled by the same factor as in figure 2.

JHEP02(2025)040

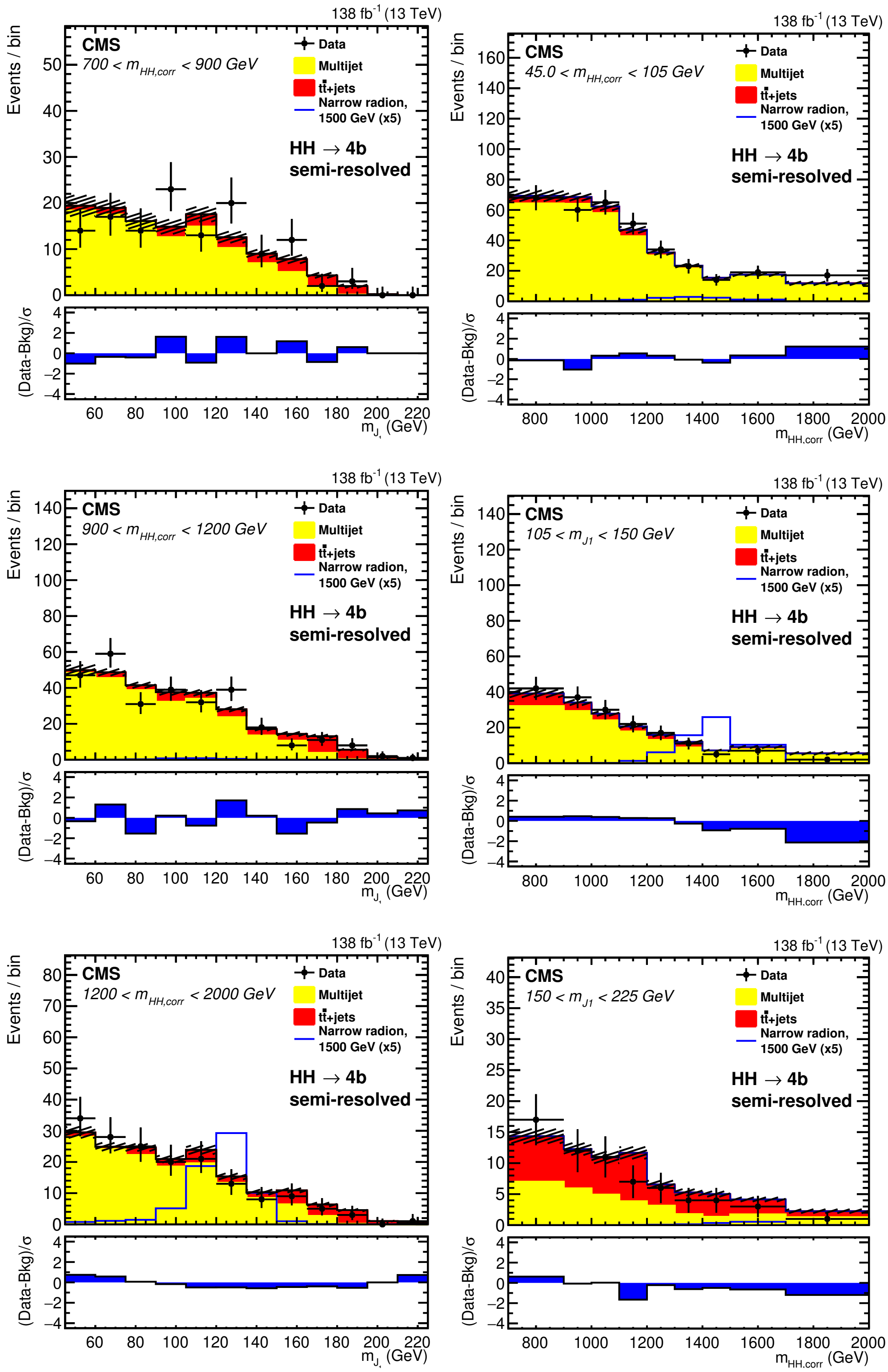

Figure 4. Slices of 2D distributions of observed events and the post-fit templates in the semi-resolved signal region, projected onto the m_{J_1} (left) and $m_{HH,corr}$ together with the signal expected for a radion of mass 1.5 TeV. The signal is scaled by the same factor as in figures 2 and 3.

JHEP02(2025)040

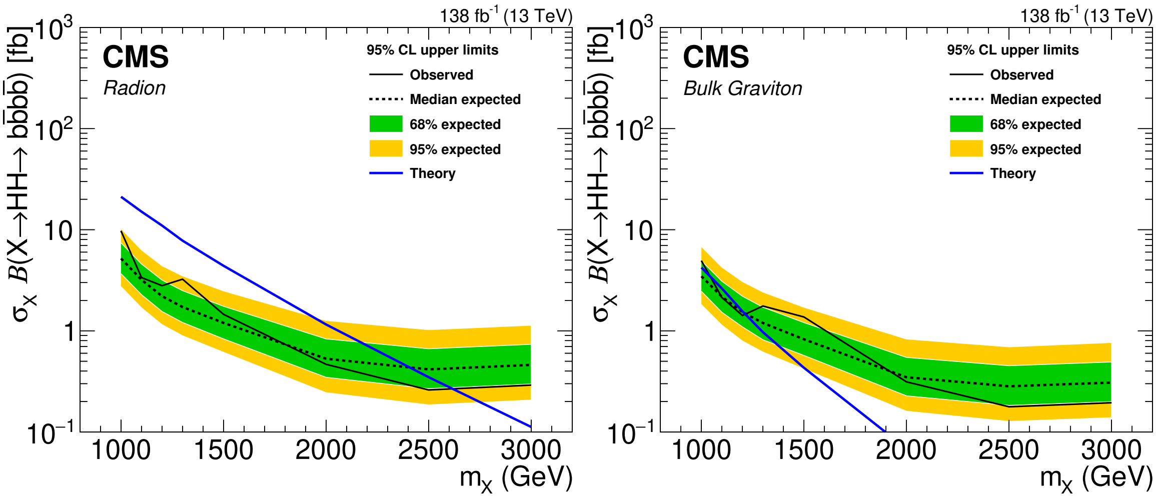

Figure 5. The observed (solid black line) and expected (dashed black line) upper limits at 95% CL on $\sigma(\mathrm{pp}\to\mathrm{X})\mathcal{B}(\mathrm{X}\to\mathrm{HH}\to\mathrm{b\bar{b}b\bar{b}})$ for a narrow spin-0 radion (left, corresponding to $\Lambda_{\mathrm{R}} = 3\,\mathrm{TeV}$) and a narrow width spin-2 bulk graviton (right, corresponding to $k/\overline{M}_{\mathrm{Pl}} = 0.5$) models. The green (yellow) bands represent one (two) standard deviations from the expected limit. The predicted theoretical cross sections for the narrow radion and bulk graviton are also shown.

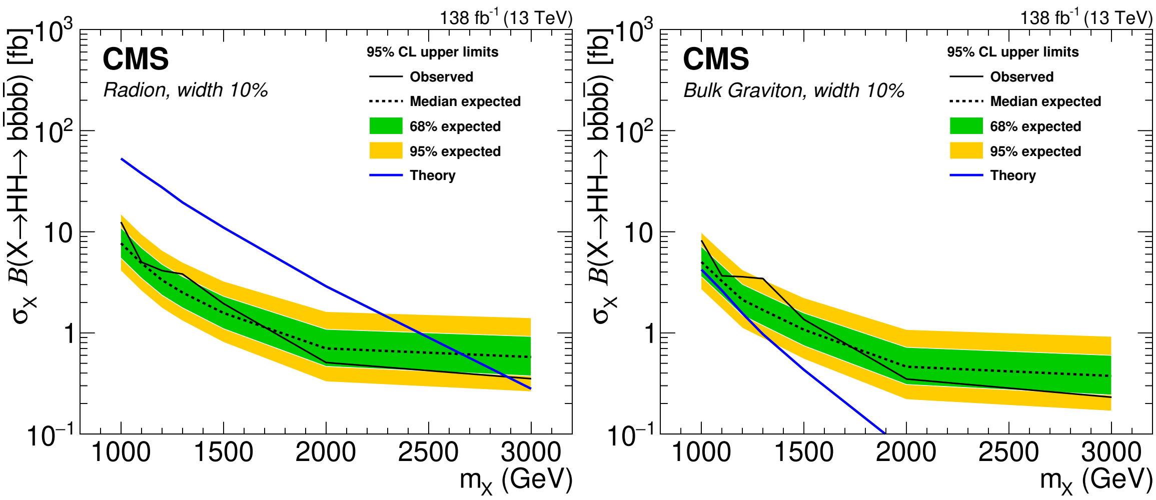

Figure 6. The observed (solid black line) and expected (dashed black line) upper limits at 95% CL on $\sigma(\mathrm{pp}\to\mathrm{X})\mathcal{B}(\mathrm{X}\to\mathrm{HH}\to\mathrm{b\bar{b}b\bar{b}})$ for the 10%-width spin-0 radion (left) and the 10%-width spin-2 bulk graviton (right) models. The green (yellow) bands represent one (two) standard deviations from the expected limit. The predicted theoretical cross sections for the 10%-width radion and bulk graviton are also shown.

a single H candidate jet. The search combines events with one H candidate jet and two b jets with events having two H candidate jets, thus adding sensitivity compared with previous analyses [46, 48]. The improvement comes from both an increase in integrated luminosity ($\approx$1.9) and an improved DeepAK8 tagger ($\approx$2.5).

The results are interpreted in terms of upper limits on the product of the production cross section for the respective resonance particles and the branching fraction to $\mathrm{HH} \to \mathrm{b\bar{b}b\bar{b}}$, at 95% confidence level. The upper limits range from 9.74 to 0.29 fb for a narrow radion and from 4.94 to 0.19 fb for a narrow bulk graviton, each having a mass of 1–3 TeV. Assuming a width of 10% for the radion and the graviton, the limits for the same masses are in the range 12.48–0.35 fb and 8.23–0.23 fb, respectively. As a result, the narrow-width graviton with m_{X} below 1.2 TeV, and narrow and 10%-width radion with masses below 2.6 TeV, and 2.9 TeV, respectively, are excluded.

Acknowledgments

We congratulate our colleagues in the CERN accelerator departments for the excellent performance of the LHC and thank the technical and administrative staffs at CERN and at other CMS institutes for their contributions to the success of the CMS effort. In addition, we gratefully acknowledge the computing centres and personnel of the Worldwide LHC Computing Grid and other centres for delivering so effectively the computing infrastructure essential to our analyses. Finally, we acknowledge the enduring support for the construction and operation of the LHC, the CMS detector, and the supporting computing infrastructure provided by the following funding agencies: SC (Armenia), BMBWF and FWF (Austria); FNRS and FWO (Belgium); CNPq, CAPES, FAPERJ, FAPERGS, and FAPESP (Brazil); MES and BNSF (Bulgaria); CERN; CAS, MoST, and NSFC (China); MINCIENCIAS (Colombia); MSES and CSF (Croatia); RIF (Cyprus); SENESCYT (Ecuador); ERC PRG, RVTT3 and MoER TK202 (Estonia); Academy of Finland, MEC, and HIP (Finland); CEA and CNRS/IN2P3 (France); SRNSF (Georgia); BMBF, DFG, and HGF (Germany); GSRI (Greece); NKFIH (Hungary); DAE and DST (India); IPM (Iran); SFI (Ireland); INFN (Italy); MSIP and NRF (Republic of Korea); MES (Latvia); LMTLT (Lithuania); MOE and UM (Malaysia); BUAP, CINVESTAV, CONACYT, LNS, SEP, and UASLP-FAI (Mexico); MOS (Montenegro); MBIE (New Zealand); PAEC (Pakistan); MES and NSC (Poland); FCT (Portugal); MESTD (Serbia); MCIN/AEI and PCTI (Spain); MOSTR (Sri Lanka); Swiss Funding Agencies (Switzerland); MST (Taipei); MHESI and NSTDA (Thailand); TUBITAK and TENMAK (Turkey); NASU (Ukraine); STFC (United Kingdom); DOE and NSF (U.S.A.).

Individuals have received support from the Marie-Curie programme and the European Research Council and Horizon 2020 Grant, contract Nos. 675440, 724704, 752730, 758316, 765710, 824093, 101115353, 101002207, and COST Action CA16108 (European Union); the Leventis Foundation; the Alfred P. Sloan Foundation; the Alexander von Humboldt Foundation; the Science Committee, project no. 22rl-037 (Armenia); the Belgian Federal Science Policy Office; the Fonds pour la Formation à la Recherche dans l'Industrie et dans l'Agriculture (FRIA-Belgium); the F.R.S.-FNRS and FWO (Belgium) under the "Excellence of Science — EOS" — be.h project n. 30820817; the Beijing Municipal Science & Technology Commission, No. Z191100007219010 and Fundamental Research Funds for the Central

Universities (China); the Ministry of Education, Youth and Sports (MEYS) of the Czech Republic; the Shota Rustaveli National Science Foundation, grant FR-22-985 (Georgia); the Deutsche Forschungsgemeinschaft (DFG), among others, under Germany's Excellence Strategy — EXC 2121 "Quantum Universe" — 390833306, and under project number 400140256 — GRK2497; the Hellenic Foundation for Research and Innovation (HFRI), Project Number 2288 (Greece); the Hungarian Academy of Sciences, the New National Excellence Program — ÚNKP, the NKFIH research grants K 131991, K 133046, K 138136, K 143460, K 143477, K 146913, K 146914, K 147048, 2020-2.2.1-ED-2021-00181, and TKP2021-NKTA-64 (Hungary); the Council of Science and Industrial Research, India; ICSC — National Research Centre for High Performance Computing, Big Data and Quantum Computing and FAIR — Future Artificial Intelligence Research, funded by the NextGenerationEU program (Italy); the Latvian Council of Science; the Ministry of Education and Science, project no. 2022/WK/14, and the National Science Center, contracts Opus 2021/41/B/ST2/01369 and 2021/43/B/ST2/01552 (Poland); the Fundação para a Ciência e a Tecnologia, grant CEECIND/01334/2018 (Portugal); the National Priorities Research Program by Qatar National Research Fund; MCIN/AEI/10.13039/501100011033, ERDF "a way of making Europe", and the Programa Estatal de Fomento de la Investigación Científica y Técnica de Excelencia María de Maeztu, grant MDM-2017-0765 and Programa Severo Ochoa del Principado de Asturias (Spain); the Chulalongkorn Academic into Its 2nd Century Project Advancement Project, and the National Science, Research and Innovation Fund via the Program Management Unit for Human Resources & Institutional Development, Research and Innovation, grant B05F650021 (Thailand); the Kavli Foundation; the Nvidia Corporation; the SuperMicro Corporation; the Welch Foundation, contract C-1845; and the Weston Havens Foundation (U.S.A.).

Data Availability Statement. Release and preservation of data used by the CMS Collaboration as the basis for publications is guided by the CMS data preservation, re-use, and open access policy.

Code Availability Statement. The CMS core software is publicly available on GitHub.

References

[1] ATLAS collaboration, *Observation of a new particle in the search for the Standard Model Higgs boson with the ATLAS detector at the LHC*, *Phys. Lett. B* **716** (2012) 1 [arXiv:1207.7214] [INSPIRE].

[2] CMS collaboration, *Observation of a new boson at a mass of 125 GeV with the CMS experiment at the LHC*, *Phys. Lett. B* **716** (2012) 30 [arXiv:1207.7235] [INSPIRE].

[3] CMS collaboration, *Observation of a new boson with mass near 125 GeV in pp collisions at* $\sqrt{s} = 7$ *and* 8 *TeV*, *JHEP* **06** (2013) 081 [arXiv:1303.4571] [INSPIRE].

[4] S. Dawson, S. Dittmaier and M. Spira, *Neutral Higgs boson pair production at hadron colliders: QCD corrections*, *Phys. Rev. D* **58** (1998) 115012 [hep-ph/9805244] [INSPIRE].

[5] S. Borowka et al., *Higgs boson pair production in gluon fusion at next-to-leading order with full top-quark mass dependence*, *Phys. Rev. Lett.* **117** (2016) 012001 [*Erratum ibid.* **117** (2016) 079901] [arXiv:1604.06447] [INSPIRE].

[6] J. Baglio et al., *Gluon fusion into Higgs pairs at NLO QCD and the top mass scheme*, *Eur. Phys. J. C* **79** (2019) 459 [arXiv:1811.05692] [INSPIRE].

[7] D.Y. Shao, C.S. Li, H.T. Li and J. Wang, *Threshold resummation effects in Higgs boson pair production at the LHC*, *JHEP* **07** (2013) 169 [arXiv:1301.1245] [INSPIRE].

[8] D. de Florian and J. Mazzitelli, *Higgs pair production at next-to-next-to-leading logarithmic accuracy at the LHC*, *JHEP* **09** (2015) 053 [arXiv:1505.07122] [INSPIRE].

[9] M. Grazzini et al., *Higgs boson pair production at NNLO with top quark mass effects*, *JHEP* **05** (2018) 059 [arXiv:1803.02463] [INSPIRE].

[10] J. Baglio et al., *$gg \to HH$: combined uncertainties*, *Phys. Rev. D* **103** (2021) 056002 [arXiv:2008.11626] [INSPIRE].

[11] LHC Higgs Cross section Working Group collaboration, *Handbook of LHC Higgs cross sections: 4. Deciphering the nature of the Higgs sector*, arXiv:1610.07922 [DOI:10.23731/CYRM-2017-002] [INSPIRE].

[12] D. de Florian and J. Mazzitelli, *Higgs boson pair production at next-to-next-to-leading order in QCD*, *Phys. Rev. Lett.* **111** (2013) 201801 [arXiv:1309.6594] [INSPIRE].

[13] J. Baglio et al., *The measurement of the Higgs self-coupling at the LHC: theoretical status*, *JHEP* **04** (2013) 151 [arXiv:1212.5581] [INSPIRE].

[14] L. Randall and R. Sundrum, *A large mass hierarchy from a small extra dimension*, *Phys. Rev. Lett.* **83** (1999) 3370 [hep-ph/9905221] [INSPIRE].

[15] L. Randall and R. Sundrum, *An alternative to compactification*, *Phys. Rev. Lett.* **83** (1999) 4690 [hep-th/9906064] [INSPIRE].

[16] W.D. Goldberger and M.B. Wise, *Modulus stabilization with bulk fields*, *Phys. Rev. Lett.* **83** (1999) 4922 [hep-ph/9907447] [INSPIRE].

[17] O. DeWolfe, D.Z. Freedman, S.S. Gubser and A. Karch, *Modeling the fifth-dimension with scalars and gravity*, *Phys. Rev. D* **62** (2000) 046008 [hep-th/9909134] [INSPIRE].

[18] C. Csaki, M. Graesser, L. Randall and J. Terning, *Cosmology of brane models with radion stabilization*, *Phys. Rev. D* **62** (2000) 045015 [hep-ph/9911406] [INSPIRE].

[19] H. Davoudiasl, J.L. Hewett and T.G. Rizzo, *Phenomenology of the Randall-Sundrum gauge hierarchy model*, *Phys. Rev. Lett.* **84** (2000) 2080 [hep-ph/9909255] [INSPIRE].

[20] C. Csaki, M.L. Graesser and G.D. Kribs, *Radion dynamics and electroweak physics*, *Phys. Rev. D* **63** (2001) 065002 [hep-th/0008151] [INSPIRE].

[21] K. Agashe, H. Davoudiasl, G. Perez and A. Soni, *Warped gravitons at the LHC and beyond*, *Phys. Rev. D* **76** (2007) 036006 [hep-ph/0701186] [INSPIRE].

[22] G.F. Giudice, R. Rattazzi and J.D. Wells, *Graviscalars from higher dimensional metrics and curvature Higgs mixing*, *Nucl. Phys. B* **595** (2001) 250 [hep-ph/0002178] [INSPIRE].

JHEP02(2025)040

[23] ATLAS collaboration, *Combination of searches for resonant Higgs boson pair production using pp collisions at $\sqrt{s} = 13$ TeV with the ATLAS detector*, Phys. Rev. Lett. **132** (2024) 231801 [arXiv:2311.15956] [INSPIRE].

[24] ATLAS collaboration, *Search for Higgs boson pair production in the $\gamma\gamma b\bar{b}$ final state using pp collision data at $\sqrt{s} = 8$ TeV from the ATLAS detector*, Phys. Rev. Lett. **114** (2015) 081802 [arXiv:1406.5053] [INSPIRE].

[25] ATLAS collaboration, *Search for Higgs boson pair production in the $b\bar{b}b\bar{b}$ final state from pp collisions at $\sqrt{s} = 8$ TeV with the ATLAS detector*, Eur. Phys. J. C **75** (2015) 412 [arXiv:1506.00285] [INSPIRE].

[26] ATLAS collaboration, *Searches for Higgs boson pair production in the $hh \to bb\tau\tau, \gamma\gamma WW^*, \gamma\gamma bb, bbbb$ channels with the ATLAS detector*, Phys. Rev. D **92** (2015) 092004 [arXiv:1509.04670] [INSPIRE].

[27] ATLAS collaboration, *Search for pair production of Higgs bosons in the $b\bar{b}b\bar{b}$ final state using proton-proton collisions at $\sqrt{s} = 13$ TeV with the ATLAS detector*, Phys. Rev. D **94** (2016) 052002 [arXiv:1606.04782] [INSPIRE].

[28] ATLAS collaboration, *Search for pair production of Higgs bosons in the $b\bar{b}b\bar{b}$ final state using proton-proton collisions at $\sqrt{s} = 13$ TeV with the ATLAS detector*, JHEP **01** (2019) 030 [arXiv:1804.06174] [INSPIRE].

[29] ATLAS collaboration, *Search for resonant and non-resonant Higgs boson pair production in the $b\bar{b}\tau^+\tau^-$ decay channel in pp collisions at $\sqrt{s} = 13$ TeV with the ATLAS detector*, Phys. Rev. Lett. **121** (2018) 191801 [*Erratum ibid.* **122** (2019) 089901] [arXiv:1808.00336] [INSPIRE].

[30] ATLAS collaboration, *Search for Higgs boson pair production in the $\gamma\gamma b\bar{b}$ final state with 13 TeV pp collision data collected by the ATLAS experiment*, JHEP **11** (2018) 040 [arXiv:1807.04873] [INSPIRE].

[31] ATLAS collaboration, *Search for Higgs boson pair production in the two bottom quarks plus two photons final state in pp collisions at $\sqrt{s} = 13$ TeV with the ATLAS detector*, Phys. Rev. D **106** (2022) 052001 [arXiv:2112.11876] [INSPIRE].

[32] ATLAS collaboration, *Search for resonant and non-resonant Higgs boson pair production in the $b\bar{b}\tau^+\tau^-$ decay channel using 13 TeV pp collision data from the ATLAS detector*, JHEP **07** (2023) 040 [arXiv:2209.10910] [INSPIRE].

[33] ATLAS collaboration, *Search for resonant pair production of Higgs bosons in the $b\bar{b}b\bar{b}$ final state using pp collisions at $\sqrt{s} = 13$ TeV with the ATLAS detector*, Phys. Rev. D **105** (2022) 092002 [arXiv:2202.07288] [INSPIRE].

[34] ATLAS collaboration, *Search for pair production of boosted Higgs bosons via vector-boson fusion in the $b\bar{b}b\bar{b}$ final state using pp collisions at $\sqrt{s} = 13$ TeV with the ATLAS detector*, Phys. Lett. B **858** (2024) 139007 [arXiv:2404.17193] [INSPIRE].

[35] CMS collaboration, *Searches for Higgs boson production through decays of heavy resonances*, arXiv:2403.16926 [INSPIRE].

[36] CMS collaboration, *Searches for heavy Higgs bosons in two-Higgs-doublet models and for $t \to ch$ decay using multilepton and diphoton final states in pp collisions at 8 TeV*, Phys. Rev. D **90** (2014) 112013 [arXiv:1410.2751] [INSPIRE].

[37] CMS collaboration, *Search for Higgs boson pair production in the $bb\tau\tau$ final state in proton-proton collisions at $\sqrt{s} = 8$ TeV*, Phys. Rev. D **96** (2017) 072004 [arXiv:1707.00350] [INSPIRE].

JHEP02(2025)040

[38] CMS collaboration, *Search for resonant pair production of Higgs bosons decaying to two bottom quark-antiquark pairs in proton-proton collisions at 8 TeV*, *Phys. Lett. B* **749** (2015) 560 [arXiv:1503.04114] [INSPIRE].

[39] CMS collaboration, *Searches for a heavy scalar boson H decaying to a pair of 125 GeV Higgs bosons hh or for a heavy pseudoscalar boson A decaying to Zh, in the final states with $h \to \tau\tau$*, *Phys. Lett. B* **755** (2016) 217 [arXiv:1510.01181] [INSPIRE].

[40] CMS collaboration, *Search for two Higgs bosons in final states containing two photons and two bottom quarks in proton-proton collisions at 8 TeV*, *Phys. Rev. D* **94** (2016) 052012 [arXiv:1603.06896] [INSPIRE].

[41] CMS collaboration, *Search for heavy resonances decaying to two Higgs bosons in final states containing four b quarks*, *Eur. Phys. J. C* **76** (2016) 371 [arXiv:1602.08762] [INSPIRE].

[42] CMS collaboration, *Search for Higgs boson pair production in events with two bottom quarks and two tau leptons in proton-proton collisions at $\sqrt{s} = 13$ TeV*, *Phys. Lett. B* **778** (2018) 101 [arXiv:1707.02909] [INSPIRE].

[43] CMS collaboration, *Search for resonant and nonresonant Higgs boson pair production in the $b\bar{b}\ell\nu\ell\nu$ final state in proton-proton collisions at $\sqrt{s} = 13$ TeV*, *JHEP* **01** (2018) 054 [arXiv:1708.04188] [INSPIRE].

[44] CMS collaboration, *Search for Higgs boson pair production in the $\gamma\gamma b\bar{b}$ final state in pp collisions at $\sqrt{s} = 13$ TeV*, *Phys. Lett. B* **788** (2019) 7 [arXiv:1806.00408] [INSPIRE].

[45] CMS collaboration, *Search for resonant pair production of Higgs bosons decaying to bottom quark-antiquark pairs in proton-proton collisions at* 13 *TeV*, *JHEP* **08** (2018) 152 [arXiv:1806.03548] [INSPIRE].

[46] CMS collaboration, *Search for a massive resonance decaying to a pair of Higgs bosons in the four b quark final state in proton-proton collisions at $\sqrt{s} = 13$ TeV*, *Phys. Lett. B* **781** (2018) 244 [arXiv:1710.04960] [INSPIRE].

[47] CMS collaboration, *Search for heavy resonances decaying into two Higgs bosons or into a Higgs boson and a W or Z boson in proton-proton collisions at 13 TeV*, *JHEP* **01** (2019) 051 [arXiv:1808.01365] [INSPIRE].

[48] CMS collaboration, *Search for production of Higgs boson pairs in the four b quark final state using large-area jets in proton-proton collisions at $\sqrt{s} = 13$ TeV*, *JHEP* **01** (2019) 040 [arXiv:1808.01473] [INSPIRE].

[49] CMS collaboration, *Search for heavy resonances decaying to a pair of Lorentz-boosted Higgs bosons in final states with leptons and a bottom quark pair at $\sqrt{s} = 13$ TeV*, *JHEP* **05** (2022) 005 [arXiv:2112.03161] [INSPIRE].

[50] CMS collaboration, *Search for a new resonance decaying into two spin-0 bosons in a final state with two photons and two bottom quarks in proton-proton collisions at $\sqrt{s} = 13$ TeV*, *JHEP* **05** (2024) 316 [arXiv:2310.01643] [INSPIRE].

[51] CMS collaboration, *Search for Higgs boson pair production in the $b\bar{b}W^+W^-$ decay mode in proton-proton collisions at $\sqrt{s} = 13$ TeV*, *JHEP* **07** (2024) 293 [arXiv:2403.09430] [INSPIRE].

[52] M. Gouzevitch et al., *Scale-invariant resonance tagging in multijet events and new physics in Higgs pair production*, *JHEP* **07** (2013) 148 [arXiv:1303.6636] [INSPIRE].

[53] CMS collaboration, *Search for a massive scalar resonance decaying to a light scalar and a Higgs boson in the four b quarks final state with boosted topology*, *Phys. Lett. B* **842** (2023) 137392 [arXiv:2204.12413] [INSPIRE].

JHEP02(2025)040

[54] A.L. Fitzpatrick, J. Kaplan, L. Randall and L.-T. Wang, *Searching for the Kaluza-Klein graviton in bulk RS models*, *JHEP* **09** (2007) 013 [hep-ph/0701150] [INSPIRE].

[55] A. Carvalho, *Gravity particles from warped extra dimensions, predictions for LHC*, arXiv:1404.0102 [INSPIRE].

[56] *HEPData record for this analysis*, https://doi.org/10.17182/hepdata.146900, (2024).

[57] CMS collaboration, *The CMS experiment at the CERN LHC*, 2008 *JINST* **3** S08004 [INSPIRE].

[58] CMS collaboration, *Performance of the CMS level-1 trigger in proton-proton collisions at* $\sqrt{s} = 13$ *TeV*, 2020 *JINST* **15** P10017 [arXiv:2006.10165] [INSPIRE].

[59] CMS collaboration, *The CMS trigger system*, 2017 *JINST* **12** P01020 [arXiv:1609.02366] [INSPIRE].

[60] CMS collaboration, *Particle-flow reconstruction and global event description with the CMS detector*, 2017 *JINST* **12** P10003 [arXiv:1706.04965] [INSPIRE].

[61] D. Contardo et al., *Technical proposal for the phase-II upgrade of the CMS detector*, CERN-LHCC-2015-010, CERN, Geneva, Switzerland (2015) [DOI:10.17181/CERN.VU8I.D59J].

[62] M. Cacciari, G.P. Salam and G. Soyez, *The anti-*k_t *jet clustering algorithm*, *JHEP* **04** (2008) 063 [arXiv:0802.1189] [INSPIRE].

[63] M. Cacciari, G.P. Salam and G. Soyez, *FastJet user manual*, *Eur. Phys. J. C* **72** (2012) 1896 [arXiv:1111.6097] [INSPIRE].

[64] CMS collaboration, *Pileup mitigation at CMS in 13 TeV data*, 2020 *JINST* **15** P09018 [arXiv:2003.00503] [INSPIRE].

[65] D. Bertolini, P. Harris, M. Low and N. Tran, *Pileup per particle identification*, *JHEP* **10** (2014) 059 [arXiv:1407.6013] [INSPIRE].

[66] CMS collaboration, *Jet energy scale and resolution in the CMS experiment in pp collisions at 8 TeV*, 2017 *JINST* **12** P02014 [arXiv:1607.03663] [INSPIRE].

[67] CMS collaboration, *Jet algorithms performance in 13 TeV data*, CMS-PAS-JME-16-003, CERN, Geneva, Switzerland (2017).

[68] J. Alwall et al., *The automated computation of tree-level and next-to-leading order differential cross sections, and their matching to parton shower simulations*, *JHEP* **07** (2014) 079 [arXiv:1405.0301] [INSPIRE].

[69] NNPDF collaboration, *Parton distributions for the LHC run II*, *JHEP* **04** (2015) 040 [arXiv:1410.8849] [INSPIRE].

[70] L.A. Harland-Lang, A.D. Martin, P. Motylinski and R.S. Thorne, *Parton distributions in the LHC era: MMHT 2014 PDFs*, *Eur. Phys. J. C* **75** (2015) 204 [arXiv:1412.3989] [INSPIRE].

[71] A. Buckley et al., *LHAPDF6: parton density access in the LHC precision era*, *Eur. Phys. J. C* **75** (2015) 132 [arXiv:1412.7420] [INSPIRE].

[72] S. Carrazza, J.I. Latorre, J. Rojo and G. Watt, *A compression algorithm for the combination of PDF sets*, *Eur. Phys. J. C* **75** (2015) 474 [arXiv:1504.06469] [INSPIRE].

[73] J. Butterworth et al., *PDF4LHC recommendations for LHC run II*, *J. Phys. G* **43** (2016) 023001 [arXiv:1510.03865] [INSPIRE].

[74] T. Sjöstrand et al., *An introduction to PYTHIA 8.2*, *Comput. Phys. Commun.* **191** (2015) 159 [arXiv:1410.3012] [INSPIRE].

[75] S. Frixione, P. Nason and G. Ridolfi, *A positive-weight next-to-leading-order Monte Carlo for heavy flavour hadroproduction*, *JHEP* **09** (2007) 126 [arXiv:0707.3088] [INSPIRE].

[76] S. Frixione, P. Nason and C. Oleari, *Matching NLO QCD computations with parton shower simulations: the POWHEG method*, *JHEP* **11** (2007) 070 [arXiv:0709.2092] [INSPIRE].

[77] S. Alioli, P. Nason, C. Oleari and E. Re, *A general framework for implementing NLO calculations in shower Monte Carlo programs: the POWHEG BOX*, *JHEP* **06** (2010) 043 [arXiv:1002.2581] [INSPIRE].

[78] S. Dulat et al., *New parton distribution functions from a global analysis of quantum chromodynamics*, *Phys. Rev. D* **93** (2016) 033006 [arXiv:1506.07443] [INSPIRE].

[79] J. Gao and P. Nadolsky, *A meta-analysis of parton distribution functions*, *JHEP* **07** (2014) 035 [arXiv:1401.0013] [INSPIRE].

[80] S. Carrazza et al., *An unbiased Hessian representation for Monte Carlo PDFs*, *Eur. Phys. J. C* **75** (2015) 369 [arXiv:1505.06736] [INSPIRE].

[81] P. Skands, S. Carrazza and J. Rojo, *Tuning PYTHIA 8.1: the Monash 2013 tune*, *Eur. Phys. J. C* **74** (2014) 3024 [arXiv:1404.5630] [INSPIRE].

[82] CMS collaboration, *Measurement of the top quark mass with lepton+jets final states using pp collisions at $\sqrt{s} = 13$ TeV*, *Eur. Phys. J. C* **78** (2018) 891 [*Erratum ibid.* **82** (2022) 323] [arXiv:1805.01428] [INSPIRE].

[83] M. Czakon and A. Mitov, *Top++: a program for the calculation of the top-pair cross-section at hadron colliders*, *Comput. Phys. Commun.* **185** (2014) 2930 [arXiv:1112.5675] [INSPIRE].

[84] GEANT4 collaboration, *GEANT4 — a simulation toolkit*, *Nucl. Instrum. Meth. A* **506** (2003) 250 [INSPIRE].

[85] J. Allison et al., *GEANT4 developments and applications*, *IEEE Trans. Nucl. Sci.* **53** (2006) 270 [INSPIRE].

[86] CMS collaboration, *Measurement of the inelastic proton-proton cross section at $\sqrt{s} = 13$ TeV*, *JHEP* **07** (2018) 161 [arXiv:1802.02613] [INSPIRE].

[87] D. Krohn, J. Thaler and L.-T. Wang, *Jet trimming*, *JHEP* **02** (2010) 084 [arXiv:0912.1342] [INSPIRE].

[88] M. Dasgupta, A. Fregoso, S. Marzani and G.P. Salam, *Towards an understanding of jet substructure*, *JHEP* **09** (2013) 029 [arXiv:1307.0007] [INSPIRE].

[89] A.J. Larkoski, S. Marzani, G. Soyez and J. Thaler, *Soft drop*, *JHEP* **05** (2014) 146 [arXiv:1402.2657] [INSPIRE].

[90] ATLAS and CMS collaborations, *Combined measurement of the Higgs boson mass in pp collisions at $\sqrt{s} = 7$ and 8 TeV with the ATLAS and CMS experiments*, *Phys. Rev. Lett.* **114** (2015) 191803 [arXiv:1503.07589] [INSPIRE].

[91] CMS collaboration, *Measurements of properties of the Higgs boson decaying into the four-lepton final state in pp collisions at $\sqrt{s} = 13$ TeV*, *JHEP* **11** (2017) 047 [arXiv:1706.09936] [INSPIRE].

[92] CMS collaboration, *Identification of heavy, energetic, hadronically decaying particles using machine-learning techniques*, 2020 *JINST* **15** P06005 [arXiv:2004.08262] [INSPIRE].

[93] CMS collaboration, *Identification of heavy-flavour jets with the CMS detector in pp collisions at 13 TeV*, 2018 *JINST* **13** P05011 [arXiv:1712.07158] [INSPIRE].

JHEP02(2025)040

[94] E. Bols et al., *Jet flavour classification using DeepJet*, 2020 *JINST* **15** P12012 [arXiv:2008.10519] [INSPIRE].

[95] CMS collaboration, *Performance of the DeepJet b tagging algorithm using 41.9 fb^{-1} of data from proton-proton collisions at 13 TeV with phase 1 CMS detector*, CMS-DP-2018-058, CERN, Geneva, Switzerland (2018).

[96] R.G. Lomax and D.L. Hahs-Vaughn, *Statistical concepts: a second course*, Taylor and Francis, Hoboken, NJ, U.S.A. (2012).

[97] K.S. Cranmer, *Kernel estimation in high-energy physics*, *Comput. Phys. Commun.* **136** (2001) 198 [hep-ex/0011057] [INSPIRE].

[98] CMS collaboration, *Precision luminosity measurement in proton-proton collisions at* $\sqrt{s} = 13$ *TeV in 2015 and 2016 at CMS*, *Eur. Phys. J. C* **81** (2021) 800 [arXiv:2104.01927] [INSPIRE].

[99] CMS collaboration, *CMS luminosity measurement for the 2018 data-taking period at* $\sqrt{s} = 13$ *TeV*, CMS-PAS-LUM-18-002, CERN, Geneva, Switzerland (2019).

[100] CMS collaboration, *CMS luminosity measurement for the 2017 data-taking period at* $\sqrt{s} = 13$ *TeV*, CMS-PAS-LUM-17-004, CERN, Geneva, Switzerland (2018).

[101] R.J. Barlow and C. Beeston, *Fitting using finite Monte Carlo samples*, *Comput. Phys. Commun.* **77** (1993) 219 [INSPIRE].

[102] J.S. Conway, *Incorporating nuisance parameters in likelihoods for multisource spectra*, in the proceedings of the *PHYSTAT 2011*, (2011) [DOI:10.5170/CERN-2011-006.115] [arXiv:1103.0354] [INSPIRE].

[103] ATLAS et al. collaborations, *Procedure for the LHC Higgs boson search combination in Summer 2011*, CMS-NOTE-2011-005, CERN, Geneva, Switzerland (2011).

[104] G. Cowan, K. Cranmer, E. Gross and O. Vitells, *Asymptotic formulae for likelihood-based tests of new physics*, *Eur. Phys. J. C* **71** (2011) 1554 [*Erratum ibid.* **73** (2013) 2501] [arXiv:1007.1727] [INSPIRE].

[105] T. Junk, *Confidence level computation for combining searches with small statistics*, *Nucl. Instrum. Meth. A* **434** (1999) 435 [hep-ex/9902006] [INSPIRE].

[106] A.L. Read, *Presentation of search results: the CL_s technique*, *J. Phys. G* **28** (2002) 2693 [INSPIRE].

JHEP02(2025)040

The CMS collaboration

Yerevan Physics Institute, Yerevan, Armenia
A. Tumasyan

Institut für Hochenergiephysik, Vienna, Austria
W. Adam, J.W. Andrejkovic, T. Bergauer, S. Chatterjee, K. Damanakis, M. Dragicevic, A. Escalante Del Valle, R. Frühwirth[1], M. Jeitler[1], N. Krammer, L. Lechner, D. Liko, I. Mikulec, P. Paulitsch, F.M. Pitters, J. Schieck[1], R. Schöfbeck, D. Schwarz, S. Templ, W. Waltenberger, C.-E. Wulz[1]

Universiteit Antwerpen, Antwerpen, Belgium
M.R. Darwish[2], E.A. De Wolf, T. Janssen, T. Kello[3], A. Lelek, H. Rejeb Sfar, P. Van Mechelen, S. Van Putte, N. Van Remortel

Vrije Universiteit Brussel, Brussel, Belgium
E.S. Bols, J. D'Hondt, M. Delcourt, H. El Faham, S. Lowette, S. Moortgat, A. Morton, D. Müller, A.R. Sahasransu, S. Tavernier, W. Van Doninck, D. Vannerom

Université Libre de Bruxelles, Bruxelles, Belgium
D. Beghin, B. Bilin, B. Clerbaux, G. De Lentdecker, L. Favart, A.K. Kalsi, K. Lee, M. Mahdavikhorrami, I. Makarenko, L. Moureaux, S. Paredes, L. Pétré, A. Popov, N. Postiau, E. Starling, L. Thomas, M. Vanden Bemden, C. Vander Velde, P. Vanlaer

Ghent University, Ghent, Belgium
T. Cornelis, D. Dobur, J. Knolle, L. Lambrecht, G. Mestdach, M. Niedziela, C. Rendón, C. Roskas, A. Samalan, K. Skovpen, M. Tytgat, B. Vermassen, L. Wezenbeek

Université Catholique de Louvain, Louvain-la-Neuve, Belgium
A. Benecke, A. Bethani, G. Bruno, F. Bury, C. Caputo, P. David, C. Delaere, I.S. Donertas, A. Giammanco, K. Jaffel, Sa. Jain, V. Lemaitre, K. Mondal, J. Prisciandaro, A. Taliercio, M. Teklishyn, T.T. Tran, P. Vischia, S. Wertz

Centro Brasileiro de Pesquisas Fisicas, Rio de Janeiro, Brazil
G.A. Alves, C. Hensel, A. Moraes, P. Rebello Teles

Universidade do Estado do Rio de Janeiro, Rio de Janeiro, Brazil
W.L. Aldá Júnior, M. Alves Gallo Pereira, M. Barroso Ferreira Filho, H. Brandao Malbouisson, W. Carvalho, J. Chinellato[4], E.M. Da Costa, G.G. Da Silveira[5], D. De Jesus Damiao, V. Dos Santos Sousa, S. Fonseca De Souza, C. Mora Herrera, K. Mota Amarilo, L. Mundim, H. Nogima, A. Santoro, S.M. Silva Do Amaral, A. Sznajder, M. Thiel, F. Torres Da Silva De Araujo[6], A. Vilela Pereira

Universidade Estadual Paulista, Universidade Federal do ABC, São Paulo, Brazil
C.A. Bernardes[5], L. Calligaris, T.R. Fernandez Perez Tomei, E.M. Gregores, D. S. Lemos, P.G. Mercadante, S.F. Novaes, Sandra S. Padula

JHEP02(2025)040

Institute for Nuclear Research and Nuclear Energy, Bulgarian Academy of Sciences, Sofia, Bulgaria
A. Aleksandrov, G. Antchev, R. Hadjiiska, P. Iaydjiev, M. Misheva, M. Rodozov, M. Shopova, G. Sultanov

University of Sofia, Sofia, Bulgaria
A. Dimitrov, T. Ivanov, L. Litov, B. Pavlov, P. Petkov, A. Petrov

Beihang University, Beijing, China
T. Cheng, T. Javaid[7], M. Mittal, L. Yuan

Department of Physics, Tsinghua University, Beijing, China
M. Ahmad, G. Bauer, C. Dozen[8], Z. Hu, J. Martins[9], Y. Wang, K. Yi[10,11]

Institute of High Energy Physics, Beijing, China
E. Chapon, G.M. Chen[7], H.S. Chen[7], M. Chen, F. Iemmi, A. Kapoor, D. Leggat, H. Liao, Z.-A. Liu[12], V. Milosevic, F. Monti, R. Sharma, J. Tao, J. Thomas-Wilsker, J. Wang, H. Zhang, J. Zhao

State Key Laboratory of Nuclear Physics and Technology, Peking University, Beijing, China
A. Agapitos, Y. An, Y. Ban, C. Chen, A. Levin, Q. Li, X. Lyu, Y. Mao, S.J. Qian, D. Wang, J. Xiao, H. Yang

Sun Yat-Sen University, Guangzhou, China
M. Lu, Z. You

Institute of Modern Physics and Key Laboratory of Nuclear Physics and Ion-beam Application (MOE) — Fudan University, Shanghai, China
X. Gao[3], H. Okawa, Y. Zhang

Zhejiang University, Hangzhou, Zhejiang, China
Z. Lin, M. Xiao

Universidad de Los Andes, Bogota, Colombia
C. Avila, A. Cabrera, C. Florez, J. Fraga

Universidad de Antioquia, Medellin, Colombia
J. Mejia Guisao, F. Ramirez, J.D. Ruiz Alvarez

University of Split, Faculty of Electrical Engineering, Mechanical Engineering and Naval Architecture, Split, Croatia
D. Giljanovic, N. Godinovic, D. Lelas, I. Puljak

University of Split, Faculty of Science, Split, Croatia
Z. Antunovic, M. Kovac, T. Sculac

JHEP02(2025)040

Institute Rudjer Boskovic, Zagreb, Croatia
V. Brigljevic, D. Ferencek, D. Majumder, M. Roguljic, A. Starodumov[13], T. Susa

University of Cyprus, Nicosia, Cyprus
A. Attikis, K. Christoforou, A. Ioannou, G. Kole, M. Kolosova, S. Konstantinou, J. Mousa, C. Nicolaou, F. Ptochos, P.A. Razis, H. Rykaczewski, H. Saka

Charles University, Prague, Czech Republic
M. Finger[13], M. Finger Jr.[13], A. Kveton

Escuela Politecnica Nacional, Quito, Ecuador
E. Ayala

Universidad San Francisco de Quito, Quito, Ecuador
E. Carrera Jarrin

Academy of Scientific Research and Technology of the Arab Republic of Egypt, Egyptian Network of High Energy Physics, Cairo, Egypt
A.A. Abdelalim[14,15], E. Salama[16,17]

Center for High Energy Physics (CHEP-FU), Fayoum University, El-Fayoum, Egypt
A. Lotfy, M.A. Mahmoud

National Institute of Chemical Physics and Biophysics, Tallinn, Estonia
S. Bhowmik, R.K. Dewanjee, K. Ehataht, M. Kadastik, S. Nandan, C. Nielsen, J. Pata, M. Raidal, L. Tani, C. Veelken

Department of Physics, University of Helsinki, Helsinki, Finland
P. Eerola, H. Kirschenmann, K. Osterberg, M. Voutilainen

Helsinki Institute of Physics, Helsinki, Finland
S. Bharthuar, E. Brücken, F. Garcia, J. Havukainen, M.S. Kim, R. Kinnunen, T. Lampén, K. Lassila-Perini, S. Lehti, T. Lindén, M. Lotti, L. Martikainen, M. Myllymäki, J. Ott, H. Siikonen, E. Tuominen, J. Tuominiemi

Lappeenranta-Lahti University of Technology, Lappeenranta, Finland
P. Luukka, H. Petrow, T. Tuuva

IRFU, CEA, Université Paris-Saclay, Gif-sur-Yvette, France
C. Amendola, M. Besancon, F. Couderc, M. Dejardin, D. Denegri, J.L. Faure, F. Ferri, S. Ganjour, P. Gras, G. Hamel de Monchenault, P. Jarry, B. Lenzi, E. Locci, J. Malcles, J. Rander, A. Rosowsky, M.Ö. Sahin, A. Savoy-Navarro[18], M. Titov, G.B. Yu

JHEP02(2025)040

Laboratoire Leprince-Ringuet, CNRS/IN2P3, Ecole Polytechnique, Institut Polytechnique de Paris, Palaiseau, France

S. Ahuja, F. Beaudette, M. Bonanomi, A. Buchot Perraguin, P. Busson, A. Cappati, C. Charlot, O. Davignon, B. Diab, G. Falmagne, S. Ghosh, R. Granier de Cassagnac, A. Hakimi, I. Kucher, J. Motta, M. Nguyen, C. Ochando, P. Paganini, J. Rembser, R. Salerno, U. Sarkar, J.B. Sauvan, Y. Sirois, A. Tarabini, A. Zabi, A. Zghiche

Université de Strasbourg, CNRS, IPHC UMR 7178, Strasbourg, France

J.-L. Agram[19], J. Andrea, D. Apparu, D. Bloch, G. Bourgatte, J.-M. Brom, E.C. Chabert, C. Collard, D. Darej, J.-C. Fontaine[19], U. Goerlach, C. Grimault, A.-C. Le Bihan, E. Nibigira, P. Van Hove

Institut de Physique des 2 Infinis de Lyon (IP2I), Villeurbanne, France

E. Asilar, S. Beauceron, C. Bernet, G. Boudoul, C. Camen, A. Carle, N. Chanon, D. Contardo, P. Depasse, H. El Mamouni, J. Fay, S. Gascon, M. Gouzevitch, B. Ille, I.B. Laktineh, H. Lattaud, A. Lesauvage, M. Lethuillier, L. Mirabito, S. Perries, K. Shchablo, V. Sordini, L. Torterotot, G. Touquet, M. Vander Donckt, S. Viret

Georgian Technical University, Tbilisi, Georgia

G. Adamov, I. Lomidze, Z. Tsamalaidze[13]

RWTH Aachen University, I. Physikalisches Institut, Aachen, Germany

V. Botta, L. Feld, K. Klein, M. Lipinski, D. Meuser, A. Pauls, N. Röwert, J. Schulz, M. Teroerde

RWTH Aachen University, III. Physikalisches Institut A, Aachen, Germany

A. Dodonova, D. Eliseev, M. Erdmann, P. Fackeldey, B. Fischer, T. Hebbeker, K. Hoepfner, F. Ivone, L. Mastrolorenzo, M. Merschmeyer, A. Meyer, G. Mocellin, S. Mondal, S. Mukherjee, D. Noll, A. Novak, A. Pozdnyakov, Y. Rath, H. Reithler, A. Schmidt, S.C. Schuler, A. Sharma, L. Vigilante, S. Wiedenbeck, S. Zaleski

RWTH Aachen University, III. Physikalisches Institut B, Aachen, Germany

C. Dziwok, G. Flügge, W. Haj Ahmad[20], O. Hlushchenko, T. Kress, A. Nowack, O. Pooth, D. Roy, A. Stahl[21], T. Ziemons, A. Zotz

Deutsches Elektronen-Synchrotron, Hamburg, Germany

H. Aarup Petersen, M. Aldaya Martin, P. Asmuss, S. Baxter, M. Bayatmakou, O. Behnke, A. Bermúdez Martínez, S. Bhattacharya, A.A. Bin Anuar, F. Blekman, K. Borras[22], D. Brunner, A. Campbell, A. Cardini, C. Cheng, F. Colombina, S. Consuegra Rodríguez, G. Correia Silva, V. Danilov, M. De Silva, L. Didukh, G. Eckerlin, D. Eckstein, L.I. Estevez Banos, O. Filatov, E. Gallo[23], A. Geiser, A. Giraldi, A. Grohsjean, M. Guthoff, A. Jafari[24], N.Z. Jomhari, A. Kasem[22], M. Kasemann, H. Kaveh, C. Kleinwort, R. Kogler, D. Krücker, W. Lange, K. Lipka, W. Lohmann[25], R. Mankel, I.-A. Melzer-Pellmann, M. Mendizabal Morentin, J. Metwally, A.B. Meyer, M. Meyer, J. Mnich, A. Mussgiller, A. Nürnberg, Y. Otarid, D. Pérez Adán, D. Pitzl, A. Raspereza,

B. Ribeiro Lopes, J. Rübenach, A. Saggio, A. Saibel, M. Savitskyi, M. Scham[26], V. Scheurer, S. Schnake, P. Schütze, C. Schwanenberger[23], M. Shchedrolosiev, R.E. Sosa Ricardo, D. Stafford, N. Tonon, M. Van De Klundert, F. Vazzoler, R. Walsh, D. Walter, Q. Wang, Y. Wen, K. Wichmann, L. Wiens, C. Wissing, S. Wuchterl

University of Hamburg, Hamburg, Germany

R. Aggleton, S. Albrecht, S. Bein, L. Benato, P. Connor, K. De Leo, M. Eich, F. Feindt, A. Fröhlich, C. Garbers, E. Garutti, P. Gunnellini, M. Hajheidari, J. Haller, A. Hinzmann, G. Kasieczka, R. Klanner, T. Kramer, V. Kutzner, J. Lange, T. Lange, A. Lobanov, A. Malara, A. Mehta, A. Nigamova, K.J. Pena Rodriguez, M. Rieger, O. Rieger, P. Schleper, M. Schröder, J. Schwandt, J. Sonneveld, H. Stadie, G. Steinbrück, A. Tews, I. Zoi

Karlsruher Institut fuer Technologie, Karlsruhe, Germany

J. Bechtel, S. Brommer, M. Burkart, E. Butz, R. Caspart, T. Chwalek, W. De Boer[†], A. Dierlamm, A. Droll, K. El Morabit, N. Faltermann, M. Giffels, J.O. Gosewisch, A. Gottmann, F. Hartmann[21], C. Heidecker, U. Husemann, P. Keicher, R. Koppenhöfer, S. Maier, M. Metzler, S. Mitra, Th. Müller, M. Neukum, G. Quast, K. Rabbertz, J. Rauser, D. Savoiu, M. Schnepf, D. Seith, I. Shvetsov, H.J. Simonis, R. Ulrich, J. Van Der Linden, R.F. Von Cube, M. Wassmer, M. Weber, S. Wieland, R. Wolf, S. Wozniewski, S. Wunsch

Institute of Nuclear and Particle Physics (INPP), NCSR Demokritos, Aghia Paraskevi, Greece

G. Anagnostou, G. Daskalakis, A. Kyriakis, A. Stakia

National and Kapodistrian University of Athens, Athens, Greece

M. Diamantopoulou, D. Karasavvas, P. Kontaxakis, C.K. Koraka, A. Manousakis-Katsikakis, A. Panagiotou, I. Papavergou, N. Saoulidou, K. Theofilatos, E. Tziaferi, K. Vellidis, E. Vourliotis

National Technical University of Athens, Athens, Greece

G. Bakas, K. Kousouris, I. Papakrivopoulos, G. Tsipolitis, A. Zacharopoulou

University of Ioánnina, Ioánnina, Greece

K. Adamidis, I. Bestintzanos, I. Evangelou, C. Foudas, P. Gianneios, P. Katsoulis, P. Kokkas, N. Manthos, I. Papadopoulos, J. Strologas

HUN-REN Wigner Research Centre for Physics, Budapest, Hungary

M. Bartók[27], G. Bencze, C. Hajdu, D. Horvath[28,29], F. Sikler, V. Veszpremi

MTA-ELTE Lendület CMS Particle and Nuclear Physics Group, Eötvös Loránd University, Budapest, Hungary

M. Csanád, K. Farkas, M.M.A. Gadallah[30], S. Lökös[31], P. Major, K. Mandal, G. Pásztor, A.J. Rádl, O. Surányi, G.I. Veres

JHEP02(2025)040

Institute of Nuclear Research ATOMKI, Debrecen, Hungary
S. Czellar, D. Fasanella, F. Fienga, J. Karancsi[27], J. Molnar, Z. Szillasi, D. Teyssier

Institute of Physics, University of Debrecen, Debrecen, Hungary
P. Raics, Z.L. Trocsanyi[32], B. Ujvari

Karoly Robert Campus, MATE Institute of Technology, Gyongyos, Hungary
T. Csorgo[33], F. Nemes[33], T. Novak

Panjab University, Chandigarh, India
S. Bansal, S.B. Beri, V. Bhatnagar, G. Chaudhary, S. Chauhan, N. Dhingra[34], R. Gupta, A. Kaur, H. Kaur, M. Kaur, P. Kumari, M. Meena, K. Sandeep, J.B. Singh, A. K. Virdi

University of Delhi, Delhi, India
A. Ahmed, A. Bhardwaj, B.C. Choudhary, M. Gola, S. Keshri, A. Kumar, M. Naimuddin, P. Priyanka, K. Ranjan, A. Shah

Saha Institute of Nuclear Physics, HBNI, Kolkata, India
M. Bharti[35], R. Bhattacharya, S. Bhattacharya, D. Bhowmik, S. Dutta, S. Dutta, B. Gomber[36], M. Maity[37], P. Palit, P.K. Rout, G. Saha, B. Sahu, S. Sarkar, M. Sharan

Indian Institute of Technology Madras, Madras, India
P.K. Behera, S.C. Behera, P. Kalbhor, J.R. Komaragiri[38], D. Kumar[38], A. Muhammad, L. Panwar[38], R. Pradhan, P.R. Pujahari, A. Sharma, A.K. Sikdar, P.C. Tiwari[38]

Bhabha Atomic Research Centre, Mumbai, India
K. Naskar[39]

Tata Institute of Fundamental Research-A, Mumbai, India
T. Aziz, S. Dugad, M. Kumar, G.B. Mohanty

Tata Institute of Fundamental Research-B, Mumbai, India
S. Banerjee, R. Chudasama, M. Guchait, S. Karmakar, S. Kumar, G. Majumder, K. Mazumdar, S. Mukherjee

National Institute of Science Education and Research, An OCC of Homi Bhabha National Institute, Bhubaneswar, Odisha, India
S. Bahinipati[40], C. Kar, P. Mal, T. Mishra, V.K. Muraleedharan Nair Bindhu[41], A. Nayak[41], P. Saha, N. Sur, S.K. Swain, D. Vats[41]

Indian Institute of Science Education and Research (IISER), Pune, India
A. Alpana, S. Dube, B. Kansal, A. Laha, S. Pandey, A. Rastogi, S. Sharma

Isfahan University of Technology, Isfahan, Iran
H. Bakhshiansohi[42], E. Khazaie[42], M. Zeinali[43]

JHEP02(2025)040

Institute for Research in Fundamental Sciences (IPM), Tehran, Iran
S. Chenarani[44], S.M. Etesami, M. Khakzad, M. Mohammadi Najafabadi

University College Dublin, Dublin, Ireland
M. Grunewald

INFN Sezione di Bari[a], Università di Bari[b], Politecnico di Bari[c], Bari, Italy
M. Abbrescia[a,b], R. Aly[a,b,45], C. Aruta[a,b], A. Colaleo[a], D. Creanza[a,c], N. De Filippis[a,c], M. De Palma[a,b], A. Di Florio[a,b], A. Di Pilato[a,b], W. Elmetenawee[a,b], F. Errico[a,b], L. Fiore[a], A. Gelmi[a,b], M. Gul[a], G. Iaselli[a,c], M. Ince[a,b], S. Lezki[a,b], G. Maggi[a,c], M. Maggi[a], I. Margjeka[a,b], V. Mastrapasqua[a,b], S. My[a,b], S. Nuzzo[a,b], A. Pellecchia[a,b], A. Pompili[a,b], G. Pugliese[a,c], D. Ramos[a], A. Ranieri[a], G. Selvaggi[a,b], L. Silvestris[a], F.M. Simone[a,b], Ü. Sözbilir[a], R. Venditti[a], P. Verwilligen[a]

INFN Sezione di Bologna[a], Università di Bologna[b], Bologna, Italy
G. Abbiendi[a], C. Battilana[a,b], D. Bonacorsi[a,b], L. Borgonovi[a], L. Brigliadori[a], R. Campanini[a,b], P. Capiluppi[a,b], A. Castro[a,b], F.R. Cavallo[a], C. Ciocca[a], M. Cuffiani[a,b], G.M. Dallavalle[a], T. Diotalevi[a,b], F. Fabbri[a], A. Fanfani[a,b], P. Giacomelli[a], L. Giommi[a,b], C. Grandi[a], L. Guiducci[a,b], S. Lo Meo[a,46], L. Lunerti[a,b], S. Marcellini[a], G. Masetti[a], F.L. Navarria[a,b], A. Perrotta[a], F. Primavera[a,b], A.M. Rossi[a,b], T. Rovelli[a,b], G.P. Siroli[a,b]

INFN Sezione di Catania[a], Università di Catania[b], Catania, Italy
S. Albergo[a,b,47], S. Costa[a,b,47], A. Di Mattia[a], R. Potenza[a,b], A. Tricomi[a,b,47], C. Tuve[a,b]

INFN Sezione di Firenze[a], Università di Firenze[b], Firenze, Italy
G. Barbagli[a], A. Cassese[a], R. Ceccarelli[a,b], V. Ciulli[a,b], C. Civinini[a], R. D'Alessandro[a,b], E. Focardi[a,b], G. Latino[a,b], P. Lenzi[a,b], M. Lizzo[a,b], M. Meschini[a], S. Paoletti[a], R. Seidita[a,b], G. Sguazzoni[a], L. Viliani[a]

INFN Laboratori Nazionali di Frascati, Frascati, Italy
L. Benussi, S. Bianco, D. Piccolo

INFN Sezione di Genova[a], Università di Genova[b], Genova, Italy
M. Bozzo[a,b], F. Ferro[a], R. Mulargia[a], E. Robutti[a], S. Tosi[a,b]

INFN Sezione di Milano-Bicocca[a], Università di Milano-Bicocca[b], Milano, Italy
A. Benaglia[a], G. Boldrini[a], F. Brivio[a,b], F. Cetorelli[a,b], F. De Guio[a,b], M.E. Dinardo[a,b], P. Dini[a], S. Gennai[a], A. Ghezzi[a,b], P. Govoni[a,b], L. Guzzi[a,b], M.T. Lucchini[a,b], M. Malberti[a], S. Malvezzi[a], A. Massironi[a], D. Menasce[a], L. Moroni[a], M. Paganoni[a,b], D. Pedrini[a], B.S. Pinolini[a], S. Ragazzi[a,b], N. Redaelli[a], T. Tabarelli de Fatis[a,b], D. Valsecchi[a,b,21], D. Zuolo[a,b]

JHEP02(2025)040

INFN Sezione di Napoli[a], Università di Napoli 'Federico II'[b], Napoli, Italy; Università della Basilicata[c], Potenza, Italy; Scuola Superiore Meridionale (SSM)[d], Napoli, Italy

S. Buontempo[a], F. Carnevali[a,b], N. Cavallo[a,c], A. De Iorio[a,b], F. Fabozzi[a,c], A.O.M. Iorio[a,b], L. Lista[a,b,48], S. Meola[a,d,21], P. Paolucci[a,21], B. Rossi[a], C. Sciacca[a,b]

INFN Sezione di Padova[a], Università di Padova[b], Padova, Italy; Università di Trento[c], Trento, Italy

P. Azzi[a], N. Bacchetta[a], D. Bisello[a,b], P. Bortignon[a], A. Bragagnolo[a,b], R. Carlin[a,b], P. Checchia[a], T. Dorigo[a], U. Dosselli[a], F. Gasparini[a,b], U. Gasparini[a,b], G. Grosso[a], S.Y. Hoh[a,b], L. Layer[a,49], E. Lusiani[a], M. Margoni[a,b], A.T. Meneguzzo[a,b], J. Pazzini[a,b], P. Ronchese[a,b], R. Rossin[a,b], F. Simonetto[a,b], G. Strong[a], M. Tosi[a,b], H. Yarar[a,b], M. Zanetti[a,b], P. Zotto[a,b], A. Zucchetta[a,b], G. Zumerle[a,b]

INFN Sezione di Pavia[a], Università di Pavia[b], Pavia, Italy

C. Aimè[a,b], A. Braghieri[a], S. Calzaferri[a,b], D. Fiorina[a,b], P. Montagna[a,b], S.P. Ratti[a,b], V. Re[a], C. Riccardi[a,b], P. Salvini[a], I. Vai[a], P. Vitulo[a,b]

INFN Sezione di Perugia[a], Università di Perugia[b], Perugia, Italy

P. Asenov[a,50], G.M. Bilei[a], D. Ciangottini[a,b], L. Fanò[a,b], M. Magherini[a,b], G. Mantovani[a,b], V. Mariani[a,b], M. Menichelli[a], F. Moscatelli[a,50], A. Piccinelli[a,b], M. Presilla[a,b], A. Rossi[a,b], A. Santocchia[a,b], D. Spiga[a], T. Tedeschi[a,b]

INFN Sezione di Pisa[a], Università di Pisa[b], Scuola Normale Superiore di Pisa[c], Pisa, Italy; Università di Siena[d], Siena, Italy

P. Azzurri[a], G. Bagliesi[a], V. Bertacchi[a,c], L. Bianchini[a], T. Boccali[a], E. Bossini[a,b], R. Castaldi[a], M.A. Ciocci[a,b], V. D'Amante[a,d], R. Dell'Orso[a], M.R. Di Domenico[a,d], S. Donato[a], A. Giassi[a], F. Ligabue[a,c], E. Manca[a,c], G. Mandorli[a,c], D. Matos Figueiredo[a], A. Messineo[a,b], M. Musich[a], F. Palla[a], S. Parolia[a,b], G. Ramirez-Sanchez[a,c], A. Rizzi[a,b], G. Rolandi[a,c], S. Roy Chowdhury[a,c], A. Scribano[a], N. Shafiei[a,b], P. Spagnolo[a], R. Tenchini[a], G. Tonelli[a,b], N. Turini[a,d], A. Venturi[a], P.G. Verdini[a]

INFN Sezione di Roma[a], Sapienza Università di Roma[b], Roma, Italy

P. Barria[a], M. Campana[a,b], F. Cavallari[a], D. Del Re[a,b], E. Di Marco[a], M. Diemoz[a], E. Longo[a,b], P. Meridiani[a], G. Organtini[a,b], F. Pandolfi[a], R. Paramatti[a,b], C. Quaranta[a,b], S. Rahatlou[a,b], C. Rovelli[a], F. Santanastasio[a,b], L. Soffi[a], R. Tramontano[a,b]

INFN Sezione di Torino[a], Università di Torino[b], Torino, Italy; Università del Piemonte Orientale[c], Novara, Italy

N. Amapane[a,b], R. Arcidiacono[a,c], S. Argiro[a,b], M. Arneodo[a,c], N. Bartosik[a], R. Bellan[a,b], A. Bellora[a,b], J. Berenguer Antequera[a,b], C. Biino[a], N. Cartiglia[a], M. Costa[a,b], R. Covarelli[a,b], N. Demaria[a], B. Kiani[a,b], F. Legger[a], C. Mariotti[a], S. Maselli[a], E. Migliore[a,b], E. Monteil[a,b], M. Monteno[a], M.M. Obertino[a,b], G. Ortona[a],

JHEP02(2025)040

L. Pacher[a,b], N. Pastrone[a], M. Pelliccioni[a], M. Ruspa[a,c], K. Shchelina[a], F. Siviero[a,b], V. Sola[a], A. Solano[a,b], D. Soldi[a,b], A. Staiano[a], M. Tornago[a,b], D. Trocino[a], A. Vagnerini[a,b]

INFN Sezione di Trieste[a], Università di Trieste[b], Trieste, Italy
S. Belforte[a], V. Candelise[a,b], M. Casarsa[a], F. Cossutti[a], A. Da Rold[a,b], G. Della Ricca[a,b], G. Sorrentino[a,b]

Kyungpook National University, Daegu, Korea
S. Dogra, C. Huh, B. Kim, D.H. Kim, G.N. Kim, J. Kim, J. Lee, S.W. Lee, C.S. Moon, Y.D. Oh, S.I. Pak, S. Sekmen, Y.C. Yang

Chonnam National University, Institute for Universe and Elementary Particles, Kwangju, Korea
H. Kim, D.H. Moon

Hanyang University, Seoul, Korea
B. Francois, T.J. Kim, J. Park

Korea University, Seoul, Korea
S. Cho, S. Choi, B. Hong, K. Lee, K.S. Lee, J. Lim, J. Park, S.K. Park, J. Yoo

Kyung Hee University, Department of Physics, Seoul, Korea
J. Goh, A. Gurtu

Sejong University, Seoul, Korea
H. S. Kim, Y. Kim

Seoul National University, Seoul, Korea
J. Almond, J.H. Bhyun, J. Choi, S. Jeon, J. Kim, J.S. Kim, S. Ko, H. Kwon, H. Lee, S. Lee, B.H. Oh, M. Oh, S.B. Oh, H. Seo, U.K. Yang, I. Yoon

University of Seoul, Seoul, Korea
W. Jang, D.Y. Kang, Y. Kang, S. Kim, B. Ko, J.S.H. Lee, Y. Lee, J.A. Merlin, I.C. Park, Y. Roh, M.S. Ryu, D. Song, I.J. Watson, S. Yang

Yonsei University, Department of Physics, Seoul, Korea
S. Ha, H.D. Yoo

Sungkyunkwan University, Suwon, Korea
M. Choi, H. Lee, Y. Lee, I. Yu

College of Engineering and Technology, American University of the Middle East (AUM), Dasman, Kuwait
T. Beyrouthy, Y. Maghrbi

Riga Technical University, Riga, Latvia
K. Dreimanis, V. Veckalns[51]

JHEP02(2025)040

Vilnius University, Vilnius, Lithuania
M. Ambrozas, A. Carvalho Antunes De Oliveira, A. Juodagalvis, A. Rinkevicius, G. Tamulaitis

National Centre for Particle Physics, Universiti Malaya, Kuala Lumpur, Malaysia
N. Bin Norjoharuddeen, Z. Zolkapli

Universidad de Sonora (UNISON), Hermosillo, Mexico
J.F. Benitez, A. Castaneda Hernandez, M. León Coello, J.A. Murillo Quijada, A. Sehrawat, L. Valencia Palomo

Centro de Investigacion y de Estudios Avanzados del IPN, Mexico City, Mexico
G. Ayala, H. Castilla-Valdez, E. De La Cruz-Burelo, I. Heredia-De La Cruz[52], R. Lopez-Fernandez, C.A. Mondragon Herrera, D.A. Perez Navarro, R. Reyes-Almanza, A. Sánchez Hernández

Universidad Iberoamericana, Mexico City, Mexico
S. Carrillo Moreno, C. Oropeza Barrera, F. Vazquez Valencia

Benemerita Universidad Autonoma de Puebla, Puebla, Mexico
I. Pedraza, H.A. Salazar Ibarguen, C. Uribe Estrada

University of Montenegro, Podgorica, Montenegro
J. Mijuskovic[53], N. Raicevic

University of Auckland, Auckland, New Zealand
D. Krofcheck

University of Canterbury, Christchurch, New Zealand
P.H. Butler

National Centre for Physics, Quaid-I-Azam University, Islamabad, Pakistan
A. Ahmad, M.I. Asghar, A. Awais, M.I.M. Awan, H.R. Hoorani, W.A. Khan, M.A. Shah, M. Shoaib, M. Waqas

AGH University of Krakow, Faculty of Computer Science, Electronics and Telecommunications, Krakow, Poland
V. Avati, L. Grzanka, M. Malawski

National Centre for Nuclear Research, Swierk, Poland
H. Bialkowska, M. Bluj, B. Boimska, M. Górski, M. Kazana, M. Szleper, P. Zalewski

Institute of Experimental Physics, Faculty of Physics, University of Warsaw, Warsaw, Poland
K. Bunkowski, K. Doroba, A. Kalinowski, M. Konecki, J. Krolikowski

JHEP02(2025)040

Laboratório de Instrumentação e Física Experimental de Partículas, Lisboa, Portugal

M. Araujo, P. Bargassa, D. Bastos, A. Boletti, P. Faccioli, M. Gallinaro, J. Hollar, N. Leonardo, T. Niknejad, M. Pisano, J. Seixas, O. Toldaiev, J. Varela

VINCA Institute of Nuclear Sciences, University of Belgrade, Belgrade, Serbia

P. Adzic[54], M. Dordevic, P. Milenovic, J. Milosevic

Centro de Investigaciones Energéticas Medioambientales y Tecnológicas (CIEMAT), Madrid, Spain

M. Aguilar-Benitez, J. Alcaraz Maestre, A. Álvarez Fernández, I. Bachiller, M. Barrio Luna, Cristina F. Bedoya, C.A. Carrillo Montoya, M. Cepeda, M. Cerrada, N. Colino, B. De La Cruz, A. Delgado Peris, J.P. Fernández Ramos, J. Flix, M.C. Fouz, O. Gonzalez Lopez, S. Goy Lopez, J.M. Hernandez, M.I. Josa, J. León Holgado, D. Moran, Á. Navarro Tobar, C. Perez Dengra, A. Pérez-Calero Yzquierdo, J. Puerta Pelayo, I. Redondo, L. Romero, S. Sánchez Navas, L. Urda Gómez, C. Willmott

Universidad Autónoma de Madrid, Madrid, Spain

J.F. de Trocóniz

Universidad de Oviedo, Instituto Universitario de Ciencias y Tecnologías Espaciales de Asturias (ICTEA), Oviedo, Spain

B. Alvarez Gonzalez, J. Cuevas, C. Erice, J. Fernandez Menendez, S. Folgueras, I. Gonzalez Caballero, J.R. González Fernández, E. Palencia Cortezon, C. Ramón Álvarez, V. Rodríguez Bouza, A. Soto Rodríguez, A. Trapote, N. Trevisani, C. Vico Villalba

Instituto de Física de Cantabria (IFCA), CSIC-Universidad de Cantabria, Santander, Spain

J.A. Brochero Cifuentes, I.J. Cabrillo, A. Calderon, J. Duarte Campderros, M. Fernandez, C. Fernandez Madrazo, P.J. Fernández Manteca, A. García Alonso, G. Gomez, C. Martinez Rivero, P. Martinez Ruiz del Arbol, F. Matorras, P. Matorras Cuevas, J. Piedra Gomez, C. Prieels, A. Ruiz-Jimeno, L. Scodellaro, I. Vila, J.M. Vizan Garcia

University of Colombo, Colombo, Sri Lanka

M.K. Jayananda, B. Kailasapathy[55], D.U.J. Sonnadara, D.D.C. Wickramarathna

University of Ruhuna, Department of Physics, Matara, Sri Lanka

W.G.D. Dharmaratna[56], K. Liyanage, N. Perera, N. Wickramage

CERN, European Organization for Nuclear Research, Geneva, Switzerland

T.K. Aarrestad, D. Abbaneo, J. Alimena, E. Auffray, G. Auzinger, J. Baechler, P. Baillon[†], D. Barney, J. Bendavid, M. Bianco, A. Bocci, C. Caillol, T. Camporesi, M. Capeans Garrido, G. Cerminara, N. Chernyavskaya, S.S. Chhibra, S. Choudhury, M. Cipriani, L. Cristella, D. d'Enterria, A. Dabrowski, A. David, A. De Roeck, M.M. Defranchis, M. Deile, M. Dobson, M. Dünser, N. Dupont, A. Elliott-Peisert, N. Emriskova, F. Fallavollita[57], A. Florent, L. Forthomme, G. Franzoni, W. Funk,

S. Ghosh, S. Giani, D. Gigi, K. Gill, F. Glege, L. Gouskos, M. Haranko, J. Hegeman, V. Innocente, T. James, P. Janot, J. Kaspar, J. Kieseler, M. Komm, N. Kratochwil, C. Lange, S. Laurila, P. Lecoq, A. Lintuluoto, K. Long, C. Lourenço, B. Maier, L. Malgeri, S. Mallios, M. Mannelli, A.C. Marini, F. Meijers, S. Mersi, E. Meschi, F. Moortgat, M. Mulders, S. Orfanelli, L. Orsini, F. Pantaleo, E. Perez, M. Peruzzi, A. Petrilli, G. Petrucciani, A. Pfeiffer, M. Pierini, D. Piparo, M. Pitt, H. Qu, T. Quast, D. Rabady, A. Racz, G. Reales Gutiérrez, M. Rovere, H. Sakulin, J. Salfeld-Nebgen, S. Scarfi, C. Schäfer, M. Selvaggi, A. Sharma, P. Silva, W. Snoeys, P. Sphicas[58], S. Summers, K. Tatar, V.R. Tavolaro, D. Treille, P. Tropea, A. Tsirou, J. Wanczyk[59], K.A. Wozniak, W.D. Zeuner

Paul Scherrer Institut, Villigen, Switzerland

L. Caminada[60], A. Ebrahimi, W. Erdmann, R. Horisberger, Q. Ingram, H.C. Kaestli, D. Kotlinski, M. Missiroli[60], L. Noehte[60], T. Rohe

ETH Zurich — Institute for Particle Physics and Astrophysics (IPA), Zurich, Switzerland

K. Androsov[59], M. Backhaus, P. Berger, A. Calandri, A. De Cosa, G. Dissertori, M. Dittmar, M. Donegà, C. Dorfer, F. Eble, K. Gedia, F. Glessgen, T.A. Gómez Espinosa, C. Grab, D. Hits, W. Lustermann, A.-M. Lyon, R.A. Manzoni, L. Marchese, C. Martin Perez, M.T. Meinhard, F. Nessi-Tedaldi, J. Niedziela, F. Pauss, V. Perovic, S. Pigazzini, M.G. Ratti, M. Reichmann, C. Reissel, T. Reitenspiess, B. Ristic, D. Ruini, D.A. Sanz Becerra, V. Stampf, J. Steggemann[59], R. Wallny

Universität Zürich, Zurich, Switzerland

C. Amsler[61], P. Bärtschi, C. Botta, D. Brzhechko, M.F. Canelli, K. Cormier, A. De Wit, R. Del Burgo, J.K. Heikkilä, M. Huwiler, W. Jin, A. Jofrehei, B. Kilminster, S. Leontsinis, S.P. Liechti, A. Macchiolo, P. Meiring, V.M. Mikuni, U. Molinatti, I. Neutelings, A. Reimers, P. Robmann, S. Sanchez Cruz, K. Schweiger, M. Senger, Y. Takahashi

National Central University, Chung-Li, Taiwan

C. Adloff[62], C.M. Kuo, W. Lin, A. Roy, T. Sarkar[37], S.S. Yu

National Taiwan University (NTU), Taipei, Taiwan

L. Ceard, Y. Chao, K.F. Chen, P.H. Chen, P.s. Chen, H. Cheng, W.-S. Hou, Y.y. Li, R.-S. Lu, E. Paganis, A. Psallidas, A. Steen, H.y. Wu, E. Yazgan, P.r. Yu

High Energy Physics Research Unit, Department of Physics, Faculty of Science, Chulalongkorn University, Bangkok, Thailand

B. Asavapibhop, C. Asawatangtrakuldee, N. Srimanobhas

Çukurova University, Physics Department, Science and Art Faculty, Adana, Turkey

F. Boran, S. Damarseckin[63], Z.S. Demiroglu, F. Dolek, I. Dumanoglu[64], E. Eskut, Y. Guler[65], E. Gurpinar Guler[65], C. Isik, O. Kara, A. Kayis Topaksu, U. Kiminsu,

JHEP02(2025)040

G. Onengut, K. Ozdemir[66], A. Polatoz, A.E. Simsek, B. Tali[67], U.G. Tok, S. Turkcapar, I.S. Zorbakir

Middle East Technical University, Physics Department, Ankara, Turkey
G. Karapinar, K. Ocalan[68], M. Yalvac[69]

Bogazici University, Istanbul, Turkey
B. Akgun, I.O. Atakisi, E. Gülmez, M. Kaya[70], O. Kaya[71], Ö. Özçelik, S. Tekten[72], E.A. Yetkin[73]

Istanbul Technical University, Istanbul, Turkey
A. Cakir, K. Cankocak[64], Y. Komurcu, S. Sen[74]

Istanbul University, Istanbul, Turkey
S. Cerci[67], I. Hos[75], B. Isildak[76], B. Kaynak, S. Ozkorucuklu, H. Sert, D. Sunar Cerci[67], C. Zorbilmez

Institute for Scintillation Materials of National Academy of Science of Ukraine, Kharkiv, Ukraine
B. Grynyov

National Science Centre, Kharkiv Institute of Physics and Technology, Kharkiv, Ukraine
L. Levchuk

University of Bristol, Bristol, United Kingdom
D. Anthony, E. Bhal, S. Bologna, J.J. Brooke, A. Bundock, E. Clement, D. Cussans, H. Flacher, J. Goldstein, G.P. Heath, H.F. Heath, L. Kreczko, B. Krikler, S. Paramesvaran, S. Seif El Nasr-Storey, V.J. Smith, N. Stylianou[77], K. Walkingshaw Pass, R. White

Rutherford Appleton Laboratory, Didcot, United Kingdom
K.W. Bell, A. Belyaev[78], C. Brew, R.M. Brown, D.J.A. Cockerill, C. Cooke, K.V. Ellis, K. Harder, S. Harper, M.-L. Holmberg[79], J. Linacre, K. Manolopoulos, D.M. Newbold, E. Olaiya, D. Petyt, T. Reis, T. Schuh, C.H. Shepherd-Themistocleous, I.R. Tomalin, T. Williams

Imperial College, London, United Kingdom
R. Bainbridge, P. Bloch, S. Bonomally, J. Borg, S. Breeze, O. Buchmuller, V. Cepaitis, G.S. Chahal[80], D. Colling, P. Dauncey, G. Davies, M. Della Negra, S. Fayer, G. Fedi, G. Hall, M.H. Hassanshahi, G. Iles, J. Langford, L. Lyons, A.-M. Magnan, S. Malik, A. Martelli, D.G. Monk, J. Nash[81], M. Pesaresi, B.C. Radburn-Smith, D.M. Raymond, A. Richards, A. Rose, E. Scott, C. Seez, A. Shtipliyski, A. Tapper, K. Uchida, T. Virdee[21], M. Vojinovic, N. Wardle, S.N. Webb, D. Winterbottom

Brunel University, Uxbridge, United Kingdom
K. Coldham, J.E. Cole, A. Khan, P. Kyberd, I.D. Reid, L. Teodorescu, S. Zahid

Baylor University, Waco, Texas, U.S.A.
S. Abdullin, A. Brinkerhoff, B. Caraway, J. Dittmann, K. Hatakeyama, A.R. Kanuganti, B. McMaster, N. Pastika, M. Saunders, S. Sawant, C. Sutantawibul, J. Wilson

Catholic University of America, Washington, DC, U.S.A.
R. Bartek, A. Dominguez, R. Uniyal, A.M. Vargas Hernandez

The University of Alabama, Tuscaloosa, Alabama, U.S.A.
A. Buccilli, S.I. Cooper, D. Di Croce, S.V. Gleyzer, C. Henderson, C.U. Perez, P. Rumerio[82], C. West

Boston University, Boston, Massachusetts, U.S.A.
A. Akpinar, A. Albert, D. Arcaro, C. Cosby, Z. Demiragli, E. Fontanesi, D. Gastler, S. May, J. Rohlf, K. Salyer, D. Sperka, D. Spitzbart, I. Suarez, A. Tsatsos, S. Yuan, D. Zou

Brown University, Providence, Rhode Island, U.S.A.
G. Benelli, B. Burkle, X. Coubez[22], D. Cutts, M. Hadley, U. Heintz, J.M. Hogan[83], T. Kwon, G. Landsberg, K.T. Lau, D. Li, M. Lukasik, J. Luo, M. Narain, N. Pervan, S. Sagir[84], F. Simpson, E. Usai, W.Y. Wong, X. Yan, D. Yu, W. Zhang

University of California, Davis, Davis, California, U.S.A.
J. Bonilla, C. Brainerd, R. Breedon, M. Calderon De La Barca Sanchez, M. Chertok, J. Conway, P.T. Cox, R. Erbacher, G. Haza, F. Jensen, O. Kukral, R. Lander, M. Mulhearn, D. Pellett, B. Regnery, D. Taylor, Y. Yao, F. Zhang

University of California, Los Angeles, California, U.S.A.
M. Bachtis, R. Cousins, A. Datta, D. Hamilton, J. Hauser, M. Ignatenko, M.A. Iqbal, T. Lam, W.A. Nash, S. Regnard, D. Saltzberg, B. Stone, V. Valuev

University of California, Riverside, Riverside, California, U.S.A.
Y. Chen, R. Clare, J.W. Gary, M. Gordon, G. Hanson, G. Karapostoli, O.R. Long, N. Manganelli, W. Si, S. Wimpenny, Y. Zhang

University of California, San Diego, La Jolla, California, U.S.A.
J.G. Branson, P. Chang, S. Cittolin, S. Cooperstein, N. Deelen, D. Diaz, J. Duarte, R. Gerosa, L. Giannini, J. Guiang, R. Kansal, V. Krutelyov, R. Lee, J. Letts, M. Masciovecchio, F. Mokhtar, M. Pieri, B.V. Sathia Narayanan, V. Sharma, M. Tadel, F. Würthwein, Y. Xiang, A. Yagil

University of California, Santa Barbara — Department of Physics, Santa Barbara, California, U.S.A.
N. Amin, C. Campagnari, M. Citron, A. Dorsett, V. Dutta, J. Incandela, M. Kilpatrick, J. Kim, B. Marsh, H. Mei, M. Oshiro, M. Quinnan, J. Richman, U. Sarica, F. Setti, J. Sheplock, P. Siddireddy, D. Stuart, S. Wang

JHEP02(2025)040

California Institute of Technology, Pasadena, California, U.S.A.

A. Bornheim, O. Cerri, I. Dutta, J.M. Lawhorn, N. Lu, J. Mao, H.B. Newman, T. Q. Nguyen, M. Spiropulu, J.R. Vlimant, C. Wang, S. Xie, Z. Zhang, R.Y. Zhu

Carnegie Mellon University, Pittsburgh, Pennsylvania, U.S.A.

J. Alison, S. An, M.B. Andrews, P. Bryant, T. Ferguson, A. Harilal, C. Liu, T. Mudholkar, M. Paulini, A. Sanchez, W. Terrill

University of Colorado Boulder, Boulder, Colorado, U.S.A.

J.P. Cumalat, W.T. Ford, A. Hassani, G. Karathanasis, E. MacDonald, R. Patel, A. Perloff, C. Savard, N. Schonbeck, K. Stenson, K.A. Ulmer, S.R. Wagner, N. Zipper

Cornell University, Ithaca, New York, U.S.A.

J. Alexander, S. Bright-Thonney, X. Chen, Y. Cheng, D.J. Cranshaw, S. Hogan, J. Monroy, J.R. Patterson, D. Quach, J. Reichert, M. Reid, A. Ryd, W. Sun, J. Thom, P. Wittich, R. Zou

Fermi National Accelerator Laboratory, Batavia, Illinois, U.S.A.

M. Albrow, M. Alyari, G. Apollinari, A. Apresyan, A. Apyan, L.A.T. Bauerdick, D. Berry, J. Berryhill, P.C. Bhat, K. Burkett, J.N. Butler, A. Canepa, G.B. Cerati, H.W.K. Cheung, F. Chlebana, K.F. Di Petrillo, J. Dickinson, V.D. Elvira, Y. Feng, J. Freeman, Z. Gecse, L. Gray, D. Green, S. Grünendahl, O. Gutsche, R.M. Harris, R. Heller, T.C. Herwig, J. Hirschauer, B. Jayatilaka, S. Jindariani, M. Johnson, U. Joshi, T. Klijnsma, B. Klima, K.H.M. Kwok, S. Lammel, D. Lincoln, R. Lipton, T. Liu, C. Madrid, K. Maeshima, C. Mantilla, D. Mason, P. McBride, P. Merkel, S. Mrenna, S. Nahn, J. Ngadiuba, V. Papadimitriou, K. Pedro, C. Pena[85], F. Ravera, A. Reinsvold Hall[86], L. Ristori, E. Sexton-Kennedy, N. Smith, A. Soha, L. Spiegel, J. Strait, L. Taylor, S. Tkaczyk, N.V. Tran, L. Uplegger, E.W. Vaandering, H.A. Weber

University of Florida, Gainesville, Florida, U.S.A.

P. Avery, D. Bourilkov, L. Cadamuro, V. Cherepanov, R.D. Field, D. Guerrero, B.M. Joshi, M. Kim, E. Koenig, J. Konigsberg, A. Korytov, K.H. Lo, K. Matchev, N. Menendez, G. Mitselmakher, A. Muthirakalayil Madhu, N. Rawal, D. Rosenzweig, S. Rosenzweig, K. Shi, J. Wang, Z. Wu, E. Yigitbasi, X. Zuo

Florida State University, Tallahassee, Florida, U.S.A.

T. Adams, A. Askew, R. Habibullah, V. Hagopian, K.F. Johnson, R. Khurana, T. Kolberg, G. Martinez, H. Prosper, C. Schiber, O. Viazlo, R. Yohay, J. Zhang

Florida Institute of Technology, Melbourne, Florida, U.S.A.

M.M. Baarmand, S. Butalla, T. Elkafrawy[17], M. Hohlmann, R. Kumar Verma, D. Noonan, M. Rahmani, F. Yumiceva

JHEP02(2025)040

University of Illinois Chicago, Chicago, U.S.A., Chicago, U.S.A.
M.R. Adams, H. Becerril Gonzalez, R. Cavanaugh, S. Dittmer, O. Evdokimov, C.E. Gerber, D.J. Hofman, A.H. Merrit, C. Mills, G. Oh, T. Roy, S. Rudrabhatla, M.B. Tonjes, N. Varelas, J. Viinikainen, X. Wang, Z. Ye

The University of Iowa, Iowa City, Iowa, U.S.A.
M. Alhusseini, K. Dilsiz[87], L. Emediato, R.P. Gandrajula, O.K. Köseyan, J.-P. Merlo, A. Mestvirishvili[88], J. Nachtman, H. Ogul[89], Y. Onel, A. Penzo, C. Snyder, E. Tiras[90]

Johns Hopkins University, Baltimore, Maryland, U.S.A.
O. Amram, B. Blumenfeld, D. Brehm, L. Corcodilos, J. Davis, A.V. Gritsan, S. Kyriacou, P. Maksimovic, J. Roskes, M. Swartz, T.Á. Vámi

The University of Kansas, Lawrence, Kansas, U.S.A.
A. Abreu, J. Anguiano, C. Baldenegro Barrera, P. Baringer, A. Bean, A. Bylinkin, Z. Flowers, T. Isidori, S. Khalil, J. King, G. Krintiras, A. Kropivnitskaya, M. Lazarovits, C. Le Mahieu, C. Lindsey, J. Marquez, N. Minafra, M. Murray, M. Nickel, C. Rogan, C. Royon, R. Salvatico, S. Sanders, E. Schmitz, C. Smith, Q. Wang, Z. Warner, J. Williams, G. Wilson

Kansas State University, Manhattan, Kansas, U.S.A.
S. Duric, A. Ivanov, K. Kaadze, D. Kim, Y. Maravin, T. Mitchell, A. Modak, K. Nam

Lawrence Livermore National Laboratory, Livermore, California, U.S.A.
F. Rebassoo, D. Wright

University of Maryland, College Park, Maryland, U.S.A.
E. Adams, A. Baden, O. Baron, A. Belloni, S.C. Eno, N.J. Hadley, S. Jabeen, R.G. Kellogg, T. Koeth, Y. Lai, S. Lascio, A.C. Mignerey, S. Nabili, C. Palmer, M. Seidel, A. Skuja, L. Wang, K. Wong

Massachusetts Institute of Technology, Cambridge, Massachusetts, U.S.A.
D. Abercrombie, G. Andreassi, R. Bi, W. Busza, I.A. Cali, Y. Chen, M. D'Alfonso, J. Eysermans, C. Freer, G. Gomez-Ceballos, M. Goncharov, P. Harris, M. Hu, M. Klute, D. Kovalskyi, J. Krupa, Y.-J. Lee, C. Mironov, C. Paus, D. Rankin, C. Roland, G. Roland, Z. Shi, G.S.F. Stephans, J. Wang, Z. Wang, B. Wyslouch

University of Minnesota, Minneapolis, Minnesota, U.S.A.
R.M. Chatterjee, A. Evans, J. Hiltbrand, Sh. Jain, M. Krohn, Y. Kubota, J. Mans, M. Revering, R. Rusack, R. Saradhy, N. Schroeder, N. Strobbe, M.A. Wadud

University of Nebraska-Lincoln, Lincoln, Nebraska, U.S.A.
K. Bloom, M. Bryson, S. Chauhan, D.R. Claes, C. Fangmeier, L. Finco, F. Golf, C. Joo, I. Kravchenko, I. Reed, J.E. Siado, G.R. Snow[†], W. Tabb, A. Wightman, F. Yan, A.G. Zecchinelli

State University of New York at Buffalo, Buffalo, New York, U.S.A.
G. Agarwal, H. Bandyopadhyay, L. Hay, I. Iashvili, A. Kharchilava, C. McLean, D. Nguyen, J. Pekkanen, S. Rappoccio, A. Williams

Northeastern University, Boston, Massachusetts, U.S.A.
G. Alverson, E. Barberis, Y. Haddad, Y. Han, A. Hortiangtham, A. Krishna, J. Li, J. Lidrych, G. Madigan, B. Marzocchi, D.M. Morse, V. Nguyen, T. Orimoto, A. Parker, L. Skinnari, A. Tishelman-Charny, T. Wamorkar, B. Wang, A. Wisecarver, D. Wood

Northwestern University, Evanston, Illinois, U.S.A.
S. Bhattacharya, J. Bueghly, Z. Chen, A. Gilbert, T. Gunter, K.A. Hahn, Y. Liu, N. Odell, M.H. Schmitt, M. Velasco

University of Notre Dame, Notre Dame, Indiana, U.S.A.
R. Band, R. Bucci, M. Cremonesi, A. Das, N. Dev, R. Goldouzian, M. Hildreth, K. Hurtado Anampa, C. Jessop, K. Lannon, J. Lawrence, N. Loukas, L. Lutton, J. Mariano, N. Marinelli, I. Mcalister, T. McCauley, C. Mcgrady, K. Mohrman, C. Moore, Y. Musienko[13], R. Ruchti, A. Townsend, M. Wayne, M. Zarucki, L. Zygala

The Ohio State University, Columbus, Ohio, U.S.A.
B. Bylsma, L.S. Durkin, B. Francis, C. Hill, M. Nunez Ornelas, K. Wei, B.L. Winer, B. R. Yates

Princeton University, Princeton, New Jersey, U.S.A.
F.M. Addesa, B. Bonham, P. Das, G. Dezoort, P. Elmer, A. Frankenthal, B. Greenberg, N. Haubrich, S. Higginbotham, A. Kalogeropoulos, G. Kopp, S. Kwan, D. Lange, D. Marlow, K. Mei, I. Ojalvo, J. Olsen, D. Stickland, C. Tully

University of Puerto Rico, Mayaguez, Puerto Rico, U.S.A.
S. Malik, S. Norberg

Purdue University, West Lafayette, Indiana, U.S.A.
A.S. Bakshi, V.E. Barnes, R. Chawla, S. Das, L. Gutay, M. Jones, A.W. Jung, D. Kondratyev, A.M. Koshy, M. Liu, G. Negro, N. Neumeister, G. Paspalaki, S. Piperov, A. Purohit, J.F. Schulte, M. Stojanovic[18], J. Thieman, F. Wang, R. Xiao, W. Xie

Purdue University Northwest, Hammond, Indiana, U.S.A.
J. Dolen, N. Parashar

Rice University, Houston, Texas, U.S.A.
D. Acosta, A. Baty, T. Carnahan, M. Decaro, S. Dildick, K.M. Ecklund, S. Freed, P. Gardner, F.J.M. Geurts, A. Kumar, W. Li, B.P. Padley, R. Redjimi, J. Rotter, W. Shi, A.G. Stahl Leiton, S. Yang, L. Zhang[91], Y. Zhang

JHEP02(2025)040

University of Rochester, Rochester, New York, U.S.A.
A. Bodek, P. de Barbaro, R. Demina, J.L. Dulemba, C. Fallon, T. Ferbel, M. Galanti, A. Garcia-Bellido, O. Hindrichs, A. Khukhunaishvili, E. Ranken, R. Taus, G.P. Van Onsem

Rutgers, The State University of New Jersey, Piscataway, New Jersey, U.S.A.
B. Chiarito, J.P. Chou, A. Gandrakota, Y. Gershtein, E. Halkiadakis, A. Hart, M. Heindl, O. Karacheban[25], I. Laflotte, A. Lath, R. Montalvo, K. Nash, M. Osherson, S. Salur, S. Schnetzer, S. Somalwar, R. Stone, S.A. Thayil, S. Thomas, H. Wang

University of Tennessee, Knoxville, Tennessee, U.S.A.
H. Acharya, A.G. Delannoy, S. Fiorendi, S. Spanier

Texas A&M University, College Station, Texas, U.S.A.
O. Bouhali[92], M. Dalchenko, A. Delgado, R. Eusebi, J. Gilmore, T. Huang, T. Kamon[93], H. Kim, S. Luo, S. Malhotra, R. Mueller, D. Overton, D. Rathjens, A. Safonov

Texas Tech University, Lubbock, Texas, U.S.A.
N. Akchurin, J. Damgov, V. Hegde, S. Kunori, K. Lamichhane, S.W. Lee, T. Mengke, S. Muthumuni, T. Peltola, I. Volobouev, Z. Wang, A. Whitbeck

Vanderbilt University, Nashville, Tennessee, U.S.A.
E. Appelt, S. Greene, A. Gurrola, W. Johns, A. Melo, K. Padeken, F. Romeo, P. Sheldon, S. Tuo, J. Velkovska

University of Virginia, Charlottesville, Virginia, U.S.A.
M.W. Arenton, B. Cardwell, B. Cox, G. Cummings, J. Hakala, R. Hirosky, M. Joyce, A. Ledovskoy, A. Li, C. Neu, C.E. Perez Lara, B. Tannenwald, S. White

Wayne State University, Detroit, Michigan, U.S.A.
N. Poudyal

University of Wisconsin — Madison, Madison, Wisconsin, U.S.A.
S. Banerjee, K. Black, T. Bose, S. Dasu, I. De Bruyn, P. Everaerts, C. Galloni, H. He, M. Herndon, A. Herve, U. Hussain, A. Lanaro, A. Loeliger, R. Loveless, J. Madhusudanan Sreekala, A. Mallampalli, A. Mohammadi, D. Pinna, A. Savin, V. Shang, V. Sharma, W.H. Smith, D. Teague, S. Trembath-Reichert, W. Vetens

Authors affiliated with an institute or an international laboratory covered by a cooperation agreement with CERN
S. Afanasiev, D. Budkouski, I. Golutvin, I. Gorbunov, V. Karjavine, V. Korenkov, A. Lanev, A. Malakhov, V. Matveev[94,95], V. Palichik, V. Perelygin, M. Savina, V. Shalaev, S. Shmatov, S. Shulha, V. Smirnov, O. Teryaev, N. Voytishin, B.S. Yuldashev[96], A. Zarubin, I. Zhizhin, G. Gavrilov, V. Golovtcov, Y. Ivanov, V. Kim[94], E. Kuznetsova[97], V. Murzin, V. Oreshkin, I. Smirnov, D. Sosnov,

JHEP02(2025)040

V. Sulimov, L. Uvarov, S. Volkov, A. Vorobyev, Yu. Andreev, A. Dermenev, S. Gninenko, N. Golubev, A. Karneyeu, D. Kirpichnikov, M. Kirsanov, N. Krasnikov, A. Pashenkov, G. Pivovarov, A. Toropin, T. Aushev, V. Epshteyn, V. Gavrilov, N. Lychkovskaya, A. Nikitenko[98], V. Popov, A. Stepennov, M. Toms, E. Vlasov, A. Zhokin, O. Bychkova, R. Chistov[94], M. Danilov[94], A. Oskin, P. Parygin, S. Polikarpov[94], V. Andreev, M. Azarkin, I. Dremin, M. Kirakosyan, A. Terkulov, A. Belyaev, E. Boos, V. Bunichev, M. Dubinin[85], L. Dudko, A. Ershov, V. Klyukhin, O. Kodolova, S. Obraztsov, M. Perfilov, S. Petrushanko, V. Savrin, V. Blinov[94], T. Dimova[94], L. Kardapoltsev[94], A. Kozyrev[94], I. Ovtin[94], O. Radchenko[94], Y. Skovpen[94], V. Kachanov, D. Konstantinov, S. Slabospitskii, A. Uzunian, A. Babaev, V. Okhotnikov, V. Borshch, V. Ivanchenko, E. Tcherniaev

Authors affiliated with an institute formerly covered by a cooperation agreement with CERN

V. Chekhovsky, A. Litomin, V. Makarenko

[†] *Deceased*
[1] *Also at TU Wien, Vienna, Austria*
[2] *Also at Institute of Basic and Applied Sciences, Faculty of Engineering, Arab Academy for Science, Technology and Maritime Transport, Alexandria, Egypt*
[3] *Also at Université Libre de Bruxelles, Bruxelles, Belgium*
[4] *Also at Universidade Estadual de Campinas, Campinas, Brazil*
[5] *Also at Federal University of Rio Grande do Sul, Porto Alegre, Brazil*
[6] *Also at The University of the State of Amazonas, Manaus, Brazil*
[7] *Also at University of Chinese Academy of Sciences, Beijing, China*
[8] *Also at Department of Physics, Tsinghua University, Beijing, China*
[9] *Also at UFMS, Nova Andradina, Brazil*
[10] *Also at Nanjing Normal University, Nanjing, China*
[11] *Now at The University of Iowa, Iowa City, Iowa, U.S.A.*
[12] *Also at University of Chinese Academy of Sciences, Beijing, China*
[13] *Also at an institute or an international laboratory covered by a cooperation agreement with CERN*
[14] *Also at Helwan University, Cairo, Egypt*
[15] *Now at Zewail City of Science and Technology, Zewail, Egypt*
[16] *Also at British University in Egypt, Cairo, Egypt*
[17] *Now at Ain Shams University, Cairo, Egypt*
[18] *Also at Purdue University, West Lafayette, Indiana, U.S.A.*
[19] *Also at Université de Haute Alsace, Mulhouse, France*
[20] *Also at Erzincan Binali Yildirim University, Erzincan, Turkey*
[21] *Also at CERN, European Organization for Nuclear Research, Geneva, Switzerland*
[22] *Also at RWTH Aachen University, III. Physikalisches Institut A, Aachen, Germany*
[23] *Also at University of Hamburg, Hamburg, Germany*
[24] *Also at Isfahan University of Technology, Isfahan, Iran*
[25] *Also at Brandenburg University of Technology, Cottbus, Germany*
[26] *Also at Forschungszentrum Jülich, Juelich, Germany*
[27] *Also at Institute of Physics, University of Debrecen, Debrecen, Hungary*
[28] *Also at Institute of Nuclear Research ATOMKI, Debrecen, Hungary*
[29] *Now at Universitatea Babes-Bolyai — Facultatea de Fizica, Cluj-Napoca, Romania*
[30] *Also at Physics Department, Faculty of Science, Assiut University, Assiut, Egypt*
[31] *Also at Karoly Robert Campus, MATE Institute of Technology, Gyongyos, Hungary*
[32] *Also at MTA-ELTE Lendület CMS Particle and Nuclear Physics Group, Eötvös Loránd University, Budapest, Hungary*

JHEP02(2025)040

[33] Also at HUN-REN Wigner Research Centre for Physics, Budapest, Hungary
[34] Also at Punjab Agricultural University, Ludhiana, India
[35] Also at Shoolini University, Solan, India
[36] Also at University of Hyderabad, Hyderabad, India
[37] Also at University of Visva-Bharati, Santiniketan, India
[38] Also at Indian Institute of Science (IISc), Bangalore, India
[39] Also at Indian Institute of Technology (IIT), Mumbai, India
[40] Also at IIT Bhubaneswar, Bhubaneswar, India
[41] Also at Institute of Physics, Bhubaneswar, India
[42] Also at Department of Physics, Isfahan University of Technology, Isfahan, Iran
[43] Also at Sharif University of Technology, Tehran, Iran
[44] Also at Department of Physics, University of Science and Technology of Mazandaran, Behshahr, Iran
[45] Now at INFN Sezione di Bari, Università di Bari, Politecnico di Bari, Bari, Italy
[46] Also at Italian National Agency for New Technologies, Energy and Sustainable Economic Development, Bologna, Italy
[47] Also at Centro Siciliano di Fisica Nucleare e di Struttura Della Materia, Catania, Italy
[48] Also at Scuola Superiore Meridionale, Università di Napoli 'Federico II', Napoli, Italy
[49] Also at Università di Napoli 'Federico II', Napoli, Italy
[50] Also at Consiglio Nazionale delle Ricerche — Istituto Officina dei Materiali, Perugia, Italy
[51] Also at Riga Technical University, Riga, Latvia
[52] Also at Consejo Nacional de Ciencia y Tecnología, Mexico City, Mexico
[53] Also at IRFU, CEA, Université Paris-Saclay, Gif-sur-Yvette, France
[54] Also at Faculty of Physics, University of Belgrade, Belgrade, Serbia
[55] Also at Trincomalee Campus, Eastern University, Sri Lanka, Nilaveli, Sri Lanka
[56] Also at Saegis Campus, Nugegoda, Sri Lanka
[57] Also at INFN Sezione di Pavia, Università di Pavia, Pavia, Italy
[58] Also at National and Kapodistrian University of Athens, Athens, Greece
[59] Also at Ecole Polytechnique Fédérale Lausanne, Lausanne, Switzerland
[60] Also at Universität Zürich, Zurich, Switzerland
[61] Also at Stefan Meyer Institute for Subatomic Physics, Vienna, Austria
[62] Also at Laboratoire d'Annecy-le-Vieux de Physique des Particules, IN2P3-CNRS, Annecy-le-Vieux, France
[63] Also at Şırnak University, Sirnak, Turkey
[64] Also at Near East University, Research Center of Experimental Health Science, Mersin, Turkey
[65] Also at Konya Technical University, Konya, Turkey
[66] Also at Izmir Bakircay University, Izmir, Turkey
[67] Also at Adiyaman University, Adiyaman, Turkey
[68] Also at Necmettin Erbakan University, Konya, Turkey
[69] Also at Bozok Universitetesi Rektörlügü, Yozgat, Turkey
[70] Also at Marmara University, Istanbul, Turkey
[71] Also at Milli Savunma University, Istanbul, Turkey
[72] Also at Kafkas University, Kars, Turkey
[73] Also at Istanbul Bilgi University, Istanbul, Turkey
[74] Also at Hacettepe University, Ankara, Turkey
[75] Also at Istanbul University — Cerrahpasa, Faculty of Engineering, Istanbul, Turkey
[76] Also at Ozyegin University, Istanbul, Turkey
[77] Also at Vrije Universiteit Brussel, Brussel, Belgium
[78] Also at School of Physics and Astronomy, University of Southampton, Southampton, United Kingdom
[79] Also at Rutherford Appleton Laboratory, Didcot, United Kingdom
[80] Also at IPPP Durham University, Durham, United Kingdom
[81] Also at Monash University, Faculty of Science, Clayton, Australia
[82] Also at Università di Torino, Torino, Italy
[83] Also at Bethel University, St. Paul, Minnesota, U.S.A.
[84] Also at Karamanoğlu Mehmetbey University, Karaman, Turkey

[85] *Also at California Institute of Technology, Pasadena, California, U.S.A.*
[86] *Also at United States Naval Academy, Annapolis, Maryland, U.S.A.*
[87] *Also at Bingol University, Bingol, Turkey*
[88] *Also at Georgian Technical University, Tbilisi, Georgia*
[89] *Also at Sinop University, Sinop, Turkey*
[90] *Also at Erciyes University, Kayseri, Turkey*
[91] *Also at Institute of Modern Physics and Key Laboratory of Nuclear Physics and Ion-beam Application (MOE) — Fudan University, Shanghai, China*
[92] *Also at Texas A&M University at Qatar, Doha, Qatar*
[93] *Also at Kyungpook National University, Daegu, Korea*
[94] *Also at another institute or international laboratory covered by a cooperation agreement with CERN*
[95] *Now at another institute or international laboratory covered by a cooperation agreement with CERN*
[96] *Also at Institute of Nuclear Physics of the Uzbekistan Academy of Sciences, Tashkent, Uzbekistan*
[97] *Also at University of Florida, Gainesville, Florida, U.S.A.*
[98] *Also at Imperial College, London, United Kingdom*

JHEP02(2025)040